ADDIS ABABA SCIENCE AND TECHNOLOGY UNIVERSITY

POST GRADUATE STUDIES

COLLEGE OF APPLIED SCIENCES

GEOLOGY DEPARTMENT

THE ROLE OF INTRUSION IN OROGENIC POLY PHASE GOLD MINERALIZATION, OKOTE AREA (SOUTHERN ETHIOPIA)

By Solomon Geda

A Thesis submitted to the department of Geology in partial fulfillment of PhD dissertation

ADDIS ABABA

March 2019

TABLE OF CONTENTS **PAGE**

LIST OF FIGURES PAGE

LIST OF PLATES PAGE

LIST OF TABLES PAGE

ABSTRACT

Granitoid hosted hypothermal gold and copper mineralization of Okote, Wayu-Boda, Gewale, Wachile and Horoto prospect areas are located in Adola belt of southern Ethiopia. Granite-granodiorite intrusive exhibit disseminated gold and copper mineralization. The ore minerals are undeformed and massive phyrite, phyrothite, chalcopyrite, malachite and azurite. Total alkali silica (TAS) discrimination diagram verified that most of the province lithologies are sub-alkaline magma in origin. The granitoid lies in the range of quartzdiorite to granite while the mafic protholith gabbro-amphibolite in composition by fulfilling the ideal setting of porphyry deposits.

AFM ternary diagram justified that the granitoids originated from tholeiitic oceanic crust. According to Sha-Chappel (1999) classification criteria, the felsic metavolcanics are I-type granite witnessing deep seated source. Alumina saturation index diagram showed that, approximately all of the metavolcanics of the study area are peraluminius in composition which are the results of partial melting of metaluminious source rock. Log-Log Y+Nb vs Rb ternary diagram is applied to address the tectonic setting of the prospects granitoid intrusive and yet verified to be volcanic arc granite. The Th-Hf-Ta ternary plot diagram for the mafic protholith also confirmed the tectonic setting to be subduction zone.

The chondrite normalized REE spider diagram of granitoids show positive Eu anomaly telling crustal contamination by the mantle wedge material overlying the melting hydrous oceanic crust during its ascent at the conveyor belt.

Most of the inclusion decrepitate (before or immediately after homogenization temperature) at 440^0C to 550^0C suggesting lack of CO_2 rich fluid and existence of juvenile hypothermal fluid. Sample for FI petrographic study clearly outlined that the fluid inclusion is type-I, characterized by moderately saline inclusion containing two phases (dominant liquid and vapor) suggesting magmatic hypothermal fluid, which is evidenced by 10-15% vapor constitute and lack of CO_2 segregation.

Considering the combined

geology, whole rock geochemistry and fluid inclusion data presented here, we can conclude that intrusive related mineralization played a vital role in Adola orogenic greenstone belt.

Key words; Gold, Copper, Granitoid, Fluid inclusion, Intrusive related, Hypothermal

ACRONYMS

AAU	Addis Ababa University
AASTU	Addis Ababa Science and Technology University
AFM	Alkali-Iron -Magnesium
AGEP	Adola Gold Exploration Project
ANS	Arabian-Nubian Shield
CA	Chemical Abrasion
CR	Crush
CHIME	Chemical Th-U –total Pb Isochron method
D	Deformation
EAO	East African Orogeny
EMRDC	Ethiopian Mineral Development Share Company
FI	Fluid Inclusion
GSE	Geological Survey of Ethiopia
HFSE	High Field Strength Element
ICP-MS	Induced coupled plasma mass spectrometry
LILE	Large Ion Lithophile Elelement
M	Metamorphism
Ma	Million annum
MB	Mozambique Belt
MGD	Metagranodiorite
MIDROC	Mohammed International Development Research and Organization Companies
MORB	Mid-oceanic ridge basalt
NMiC	National Mining Corporation
Qv	Quartz vein
REE	Rare earth elements
SES	Southern Ethiopian Shield
TAS	Total Alkali Silica
XRF	X-ray fluorescence

CHAPTER ONE

1. INTRODUCTION

1.1. Location and accessibility

Okote gold project, owned by National Mining Corporation P.L.C, is one of the primary gold resources under feasibility study. In 1996, NMiC carried out its gold exploration in Dawa Digati (Okote) project, with a scope of exploration focus. Profitability of this deposit is determined by a number of factors and parameters including geological and geotechnical properties of both ore body and the enclosing materials. Lithological, structural and compositional makeup of the deposit has significant influence on the economic recovery of target commodity/gold. The two interrelated mineralizations of orogenic gold belts namely intrusive related and shear hosted vein type deposits are outlined by academic researcher (Solomon, 2015).

Okote prospect area is located in Hallo kebele, Melka Soda wereda, west Guji zone of Oromia regional state in southern Ethiopia (Figure 1). It is located, approximately 610km south of Addis Ababa or 100km south of LegaDembi gold mine. It is bounded by coordinates; 38°46‘00’’-38°46‘45’’E and 5°06’00’’-5°07‘20’’N which is about 48km^2 in areal extent.

The copper and base metal prospect license areas: Gewale, Wachile and Horoto are found 70 km south while Wayu Boda project was once owned by Alecto Minerals plc is 24km south of Okote. The mentioned prospects are found in southern Ethiopia under the Oromia national regional administrative state, within the Arero district of Borena zone. The prospect areas have similarity of mineralization enriched in gold and copper hosted by porphyritic granitoids aligned in a relatively sub parallel position to Legadembi-Aflata shear zone.

Okote prospect area is accessed through asphalt road of 470 km up to Bule-Hora town and gravel road of 130 km from Bule-Hora town up to the study area. Pavement roads connect the prospect area and exploration sites of a number of metallogenic provinces. A little operational infrastructure is currently available on site and the majority of the license area is covered with farms although scattered manual mining operations are present. Several roads in the area have been constructed for the purpose of exploration. Almost all communities outside of Hallo settlement are inaccessible by vehicles other than motorbikes; consequently donkeys are the main form of transportation for goods and supplies.

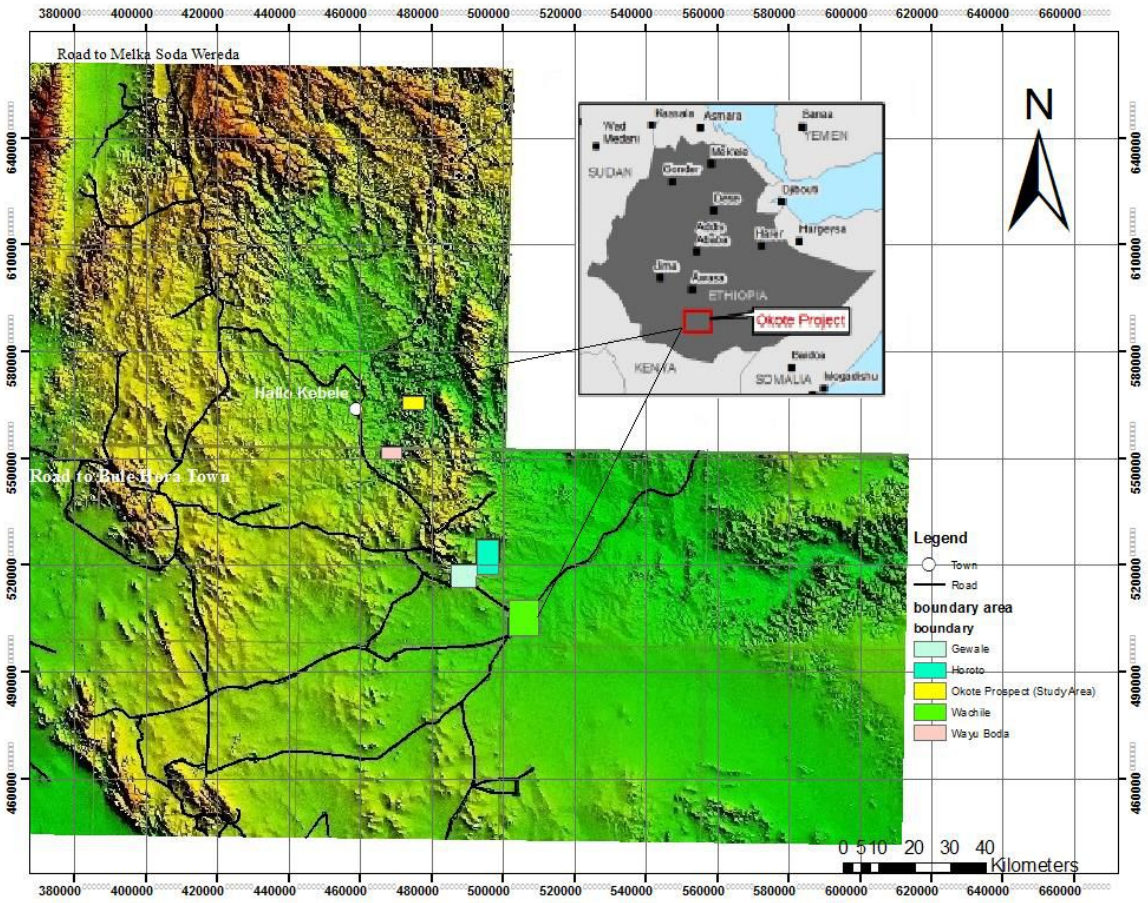

Figure1. Location map of study area

1.2. Physiography and climate

The study area is located in the southerly part of the country in Ethiopian high lands. The prospect is extremely hilly with numerous steep ridges, incised valleys and deep gorges bounding the project area to the south, east and north-west. The project site itself ranges in elevation from approximately 1,200 to 1,500 masl. The project area is incised by several seasonal drainage lines and rivers, which can run from north to south.

Ethiopia is located in the tropics and is characterized by relatively high temperatures and humidity that remain fairly constant throughout the year. The Oromia region has a mean annual rainfall of 410-820mm with noticeable variability from year (Ethiopia Government portal, 2012). The climatic types prevailing in the Oromia region can be grouped into three major activities: dry climate, semi-arid climate and temperate climate. The project area is located in the semi-arid climate characterized by

two rainy seasons peaking in May and October. In this climatic region, minimum and maximum temperatures remain approximately 10^0C and 25^0C respectively.

Okote prospect area is in the Genale-Dawa basin and is characterized by steep valleys and rugged terrain. Channels in the project impacted areas are ephemeral, with flow generally occurring during the rainy season or following large storm events. The Geleba river forms a tributary of the Dawa river approximately 8km north-east of the study area and typically flows only during the wet season. The Aflata river is located to the north of the project site and flows in a west to easterly direction into the Dawa river approximately 800m before the confluence with the Dawa and Geleba. The Aflata and Dawa rivers typically flow for the majority of the year, however it is understood that Aflata has rare dry spells during very dry years.

1.3. Vegetation and wildlife

The project area is vegetated with a range of trees, shrubs and plants typical of a semi-arid climate. Low agricultural productivity in the locality is a feature not only of limited rainfall, but also of the rocky terrain associated with thin and impoverished soils. Within the project area soil appear to be generally low in available nitrogen and phosphorous and can not produce high crop yields unless these are supplied.

There is evidence of human pressure, resulting from habitation and artisanal mining activities that have a degrading effect on riparian habitats within the project area. There is a low potential for medium and large mammals due to the pressure from human activities on habitats, however, there is a medium-high density of bats in the area. The prospect area is home of several bird species, including Abyssinian Oriole.

1.4. Socio-economy

Melka Soda wereda consists of 14 Kebeles and in the Halo Kebele, where the study area is located, the total population is 4,914. Out of this 47.3% are men and 52.7% are women. In Halo kebele there are 700 households. These means the average household has seven inhabitants.

The local inhabitants are Guji tribes of the Oromo nationality. Pastoralism and beekeeping is combined with artisanal and small scale mining. Other economic activities at the wereda and kebele level include trade, collection of non-timber forest products (such as gum), production of wooden items and production of handicrafts.

CHAPTER TWO

2. SYNOPSIS

2.1. Literature review

The precambrian terrain of Africa consists of Archean cratons welded together by proteozoic mobile belts. The precambrian of eastern Africa, in particular, is comprised of genetically-related mobile belts known as mozambique belt (MB) in the south, and the Arabian-Nubian shield (ANS) in the north. The two mobile belts together form the east African orogen. The East African Orogen, extends from southern Israel, Sinai and Jordan in the north to Mozambique and Madagascar in the south, and is one of the worldś largest Neoproterozoic to Cambrian orogenic complex. It extends for about 6000Km along the eastern flank of Africa (Figure 2.1). The Northern part of EAO is the Arabian-Nubian Shield which is composed largely of low grade juvenile Neoproterozoic crust whereas the southern part is predominantly high grade rocks which incorporates partly reworked older crust. The EAO marks one of earth's greatest collision zone, formed during the collision of East and West Gondwana and marks the disappearance of Mozambique ocean (Stern, 2007). It consists of deformed and metamorphosed rocks of the Arabian-Nubian Shield (ANS) in the north and higher grade and more strongly deformed rocks of Mozambique Belt in the south (Abdelselam and Stern, 1997).

The Juvenile Arabian-Nubian shield of the EAO was thought to have developed through the process of island arc-back arc formation and subsequent lateral accretion which finally produced cratonized crust during the neo-proterozoic (850-650 ma) (Gas,1981, Vial 1983, Stern 1994). The southern EOA, the Mozambique belt, on other hand was interpreted as resulted due to continent-continent collusion, similar to the formation of phanerozoic Himalayan mountain belt (Dewit & Chewaka 1981). The two components were developed simultaneously as a result of closure of Mozambique ocean under oblique NW-SE convergence in the time span of 850-550ma. The closure of the Mozambique ocean by island arc formation, collision of the arcs and lateral accretion is marked by ophiolite decorated suture zones in the Arabian-Nubian shield (Abdelselam and Stern, 1997, Shakleton 1997, Berhe 1990); and by crustal staking by thrust faulting and medium to high grade metamorphic zones in the Mozambique belt (MB). The final stage of EAO is characterized by lateral

extension (escape tectonics) to the north along orogen parallel strike slip shear zones. The escape tectonics is accompanied by across orogen (NW-SE) trending accumulative extension zones (Stern 1994). These orogenic related magmatism, tectonism and metamorphism control the overall stratigraphic-structural, metamorphic disposition and mineral deposition in the belt.

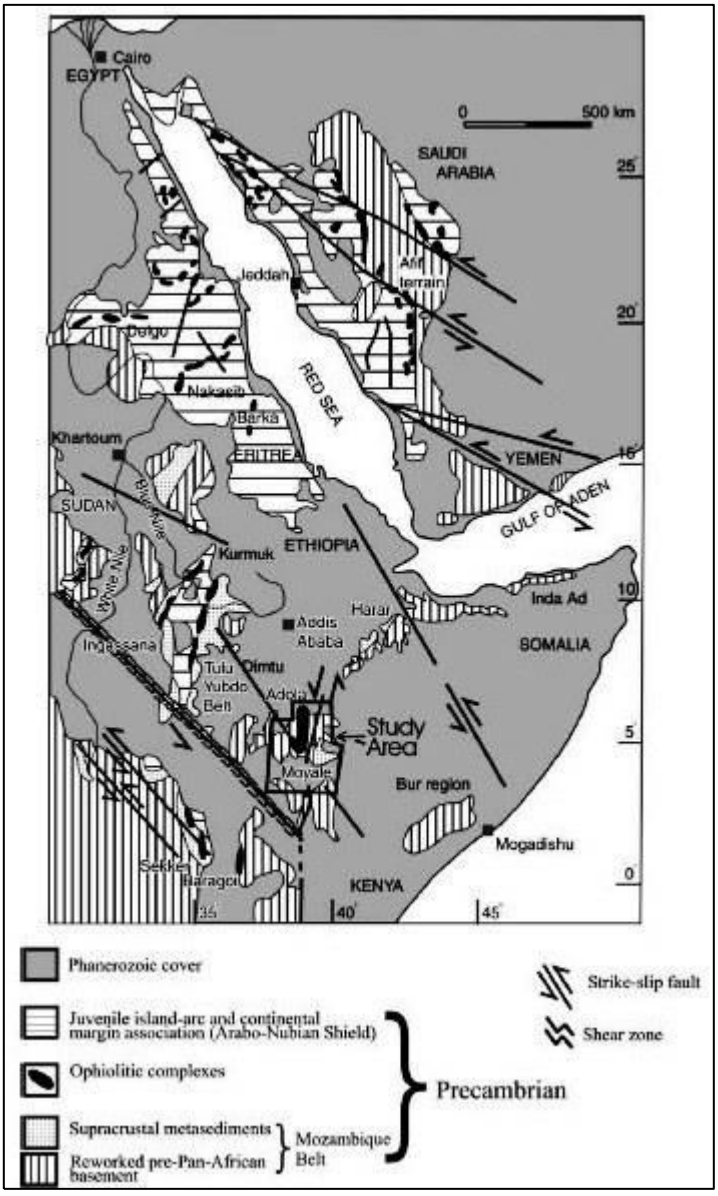

Figure2.1.Geology map of NE Africa, modified after Worku and Schandelmeier (1996) and Shackleton (1997), showing the Precambrian of southern Ethiopia within the confines of the east African Orogen

The Precambrian geology of Ethiopia is covered by low to medium grade metamorphic rocks of the Arabian Nubian shield, together with the high grade metamorphic rocks of Mozambique. The

coexistence of these two major metamorphic rock types in the southern part of the country is defined as Southern Ethiopian Shield (SES). The Southern Ethiopian geology is composed of inter-fingering of Neoproterozoic largely greenschist facies juvenile crust of the Arabian-Nubian Shield represented the Adola group of rocks mainly; Kenticha, Megado, and Bulbul terranes and the higher grade metamorphosed rocks of the Mozambique Belt represented by the Alghe terrane (Abdelselam and Stern.; 1997).

Efforts aimed at the discovery of economic deposit of gold in the Adola dates back to 1930's when Italian companies discovered gold in Shakisso area. Early exploration was concentrated mainly on placer gold exploration and development but also a significant amount of work was conducted to elaborate the geology of area and primary economic mineral deposits. A comprehensive study of the area involving geological mapping, reconnaissance mineral exploration, prospecting and detail exploration for primary and placer gold and rare earth elements deposits was conducted by Adola Gold Exploration Project (AGEP) between 1979-1981, Shiferaw et al (1985), Kozrev et al (1985), Shilehov et al (1985) and Derefeev et al (1985). These works have produced geological, geochemical and geomorphological maps of the area and discovered several metallic and non-metallic mineral occurrences. The results include more than 30 primary gold occurrences and geochemical haloes. The LegaDembi primary gold deposit was the major discovery of the project but other discoveries include the Megado-Serdo and Dawa-Digati gold anomalies. Extensive geological work has been carried out by geological survey of Ethiopia (GSE) on the Precambrian basement rocks of southern Ethiopia since its establishment in 1968. As a result geological map of southern Ethiopia especially of Adola belt is available at scale of 1:50,000. The map depicts valuable and detailed information which can enhance further understanding of the tectonic evolution of the area and mineralization potential.

Gilboy (1979), Chater (1971) and Woldehaimanot and Behrmann (1995) have recognized two main metamorphic events in Adola Belt. M1 affects basement units prior to the major thrusting and M2 which is syn-to postdeformation affecting basement units and the Adola Fold and Thrust Belt. The metamorphic grade increases from lower and mid amphibolites facies in the NW to upper amphibolites and lower granulitesfacies in the SE of the gneissic terrain (Gilboy, 1970). Beraki et al., 1989 suggested two metamorphic cycles separated by a period of uplift and erosion (as cited in Abu Wube, 2005).

Five tectonothermal events in the evolution of the East African Orogen(See Figure 2) are recognized in the Precambrian of southern Ethiopia: the Adola (1157± 2 to 1030± 40 Ma), Bulbul–Awata (876 5 Ma), Megado (800–750 Ma), Moyale (700–550 Ma) and Berguda (550–500 Ma) tectonothermal events (Yibas 2002). This data along with other studies from north and western Ethiopia refuted the three fold stratigraphy classification of Kazmin (1971, 1975); the lower complex, the middle complex and upper complex of the Precambrian basement of Ethiopia.

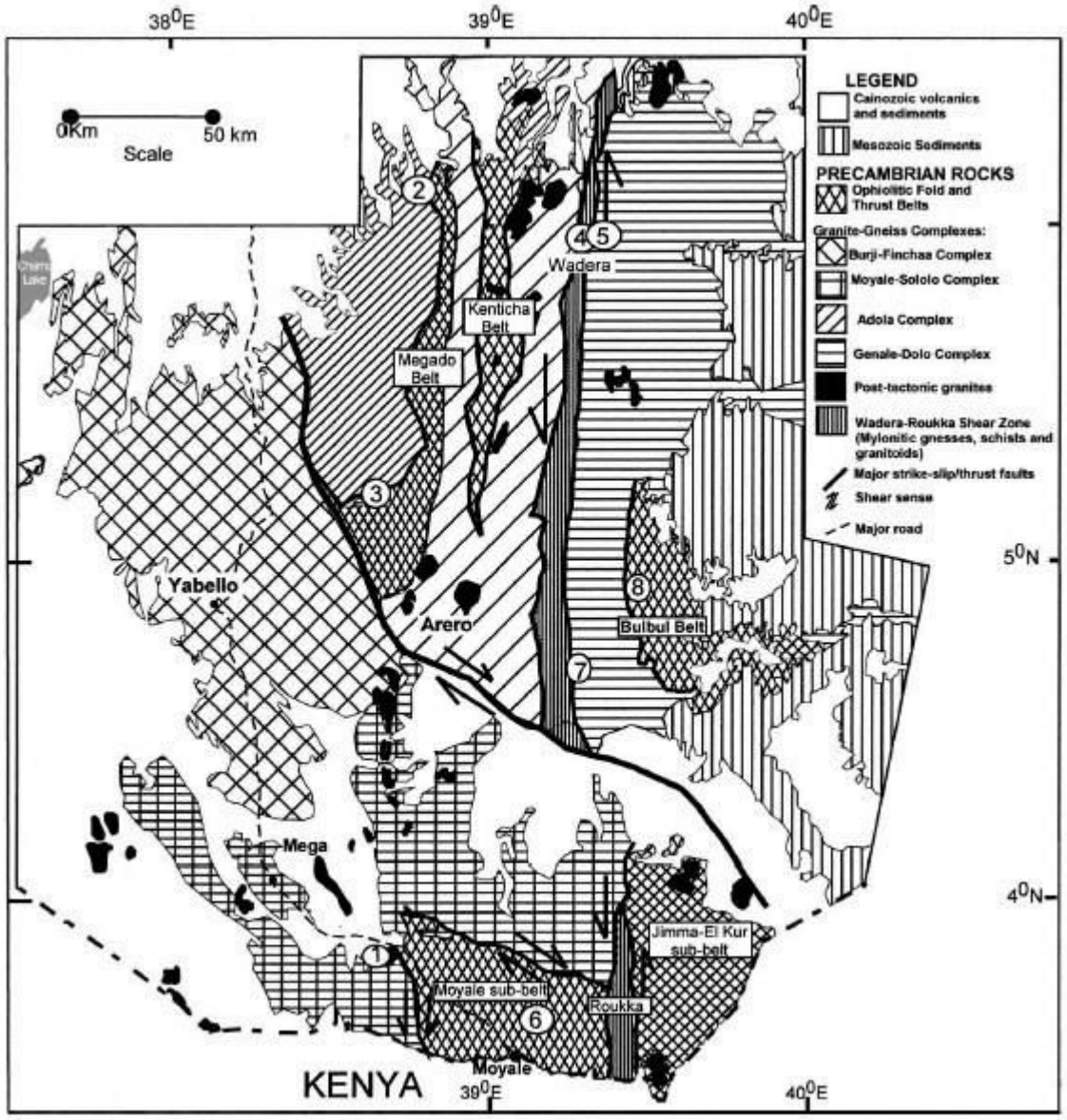

Figure2.2. Tectonostatigraphic map of the Precambrian geology of southern Ethiopia with project area location (Yibas, 2002)

Due to the complexity of deformation, the Adola gold belt has been sub-divided into five lithostructural domains namely; the Western Gneissic Domain; the Metavolcano sedimentary Domain (Megado greenstone belt);the Burjiji-Gariboro Domain; the Ultrabasic Domain; and (Kenticha greenstone belt) and the Eastern Gneissic Domain. Early works in the area concluded that, the N-S trending tectonic shear zone which is presumed to be phase of EOA associated with escape tectonic might have controlled the distribution of the five lithostructural domains of Adola gold belt. The low grade greenstone belts known as Megado greenstone belt (known for its gold and base metal mineralization) and Kenticha greenstone belt (known REE &gemstones mineralization) form Grabens, while the high grade Gneissic terrains, known as central (Gariboro/ Burjiji) and Western and Eastern basements form horsts (Kozyrev et al. 1988). However most recent works eg. Asrat, (2001) regroup the southern Ethiopian metamorphic terrain into two major blocks: the volcano-sedimentary terrain and the Gneissic-migmatitic terrain separated by tectonic contacts marked by dismembered numerous Ophiolitic rocks.

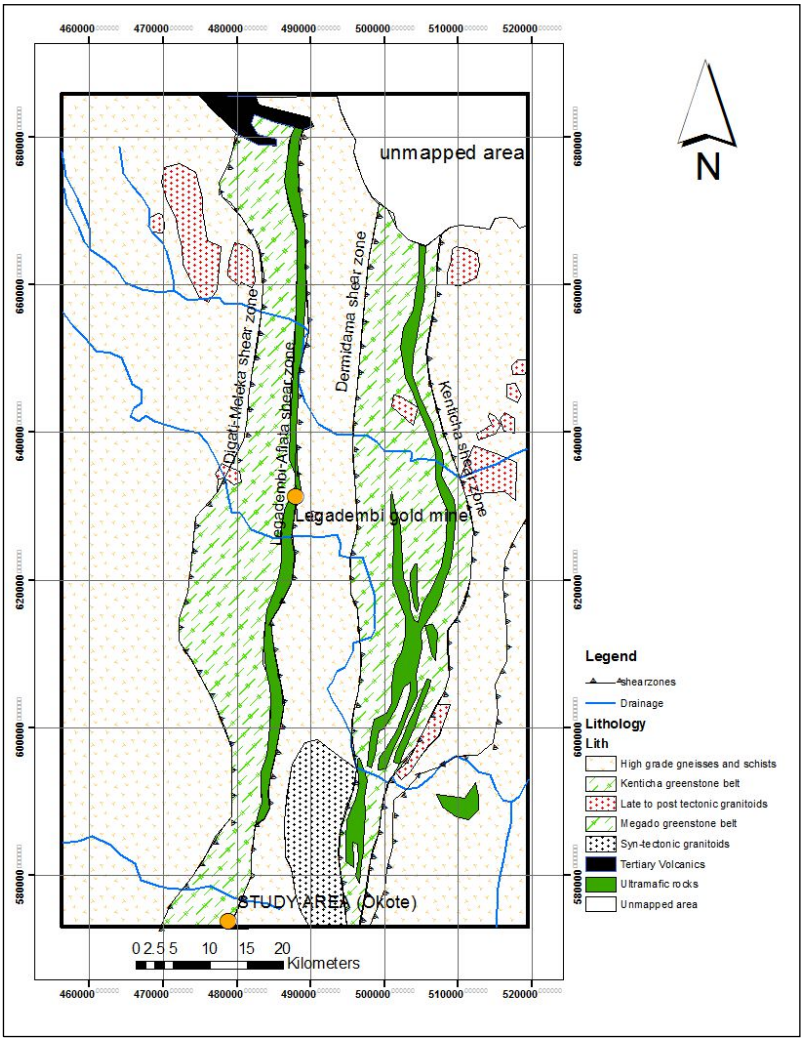

Figure2.3. Five Litho-structural domains of Adola belt (Worku and Schandelmeier, 1996)

Structural study of the Adola belt shows that most of its known and potential Au deposits in southern Ethiopia occur in quartz veins which are localized within shear contacts between lithological units, and along major shear zones that divide the Adola belt into different lithostructural domains. Analysis of the shear zone-related ore bodies and their host rocks indicates that Au mineralization in the Adola belt is pre-dated by two stages of deformation and a regional prograde metamorphism. The first deformation event (D1) is a fold-and-thrust event which is characterized by low-angle thrusts, associated recumbent folds and axial planar S~ foliation, and is related to nappe-style deformation. The second event (D2) has folded and/or reactivated the thrust-related structures and formed upright folds and high-angle reverse shear zones and is related to the collision event.

Gold mineralization is thought to have occurred over a prolonged deformation history and is closely related to alteration, retrograde greenschist facies metamorphism and brittle-ductile deformation of late D2 and D3 transpressional shear zones that accommodate regional shortening both by crustal thickening and lateral displacement. The increase in Au concentration along the Megado greenschist-facies metavolcano-sedimentary terrane as compared to the gneissic rocks is related to its development in a rapid extensional zone and subsidence environment in an inter-arc/back-arc setting and the mineralization is genetically related to the subduction event (Worku, 1997).

The study area is located in southern Ethiopia at the southern extension of the Adola gold belt (Figure 2.3). The geology of Okote prospect is part of the southern extension of the metavolcano-sedimentary rocks of the Adola belt. It lies within Megado lithostructural domain of Worku and Schandelmeier (1996) or within the volcano-sedimentary domain of Yibas (2002) and Asrat (2001).

About 2 km east of the prospect area, one can see the Burjiji–Gariboro gneiss (Ranu granitic gneiss), while the western side of the prospect is characterized by intercalation of metagranodiorite and amphibolite. The Burjiji-Gariboro gneiss marking the eastern contact of the Megado-Volcano sedimentary belt is a prominent unit that stretches almost throughout the length of the belt. Lithologically, the area is comprised of schists mainly chlorite- amphibole, carbonate-chlorite, talc-tremolite and associated intrusive ranging from granodiorite to metagabbro of different compositions.

Litholohgical and structural evidences observed during the field exploration works of the prospect outlined that biotite-quartzofeldspathic gneiss and amphibole-quartzofeldspathic gneiss represent the lowest stratigraphic units by showing a tectonic contact with the overlying mafic-ultramafic rocks (meta-ultramafic rocks, amphibolite, metagabro, and meta-volcanic rocks) and latter on intruded by intermediate to felsic /syn/post tectonic intrusion.

The project area is generally characterized by lower amphibolite to upper greenschist facies metamorphism of the meta-volcano-sedimentary assemblages. The main lithologies are typically schists rich in talc and chlorite with significant amount of sericite, tremolite and actinolite.

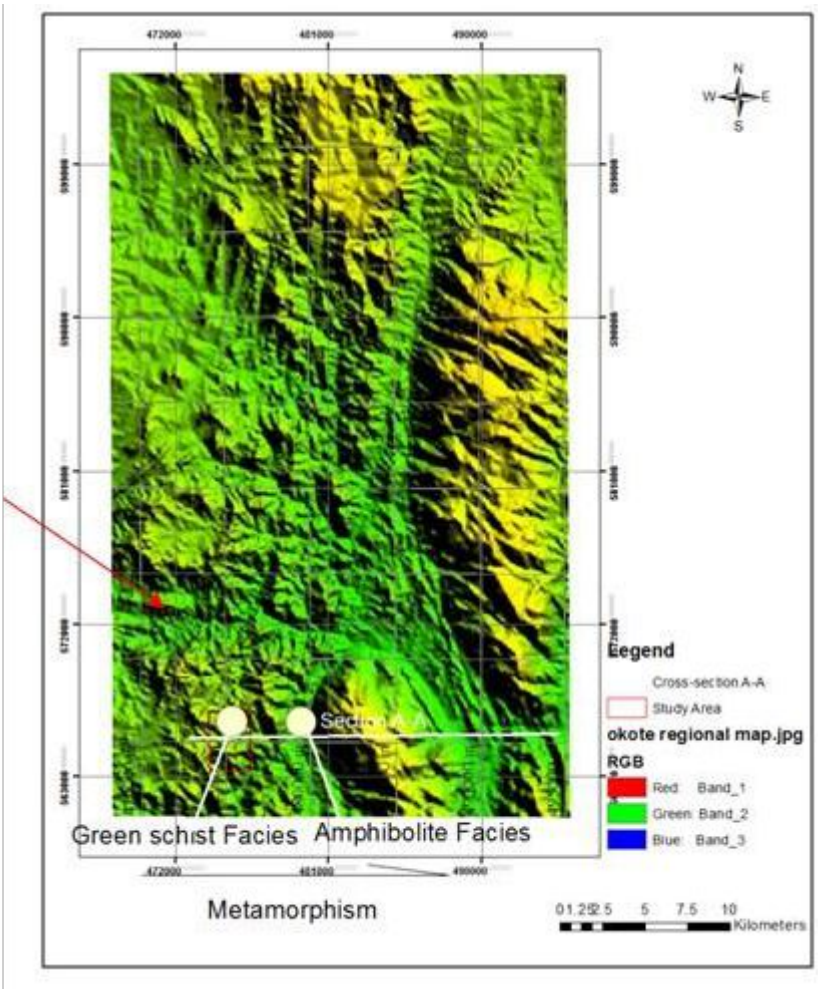

Figure2.4. Metamorphism across the study area (DEM data from Global Mapper)

Grade of metamorphism increases while moving from the study area to the east, with metamorphism disruption by north-south trending shear zone.The mafic-ultramafic constitute the hanging wall of the thrust surface and are schistose with intensity of metamorphism decrease away from the thrust surface.

As can be seen from the map area is located in a major shear zone where lithologies are variably metamorphosed and structural control is important. The three deformation events (D1, D2& D3) are similar to what Worku (1997) have described while E-W running D4 structure is local to Okote and is hosting barren milky white quartz vein (E-W stretch shown by red arrow of Figure 2.4) Abu Wube (2005).

The N-S stretches of the prospect are far away from the regional shear zone, they are considered to be splays of Legadembi–Aflata shear zones. The Legadembi-Aflata shear zone is characterized by strongly deformed rocks and form topographically low as compared to the surrounding areas (Figure 2.5).

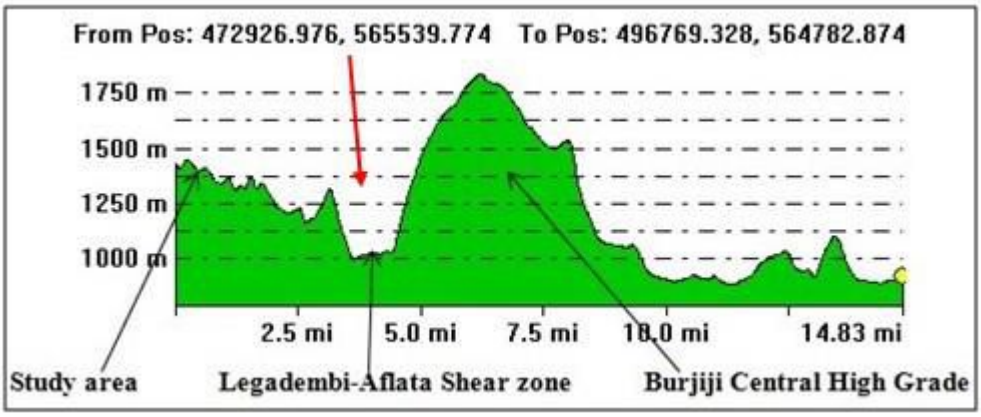

Figure2.5. Shear zone demonstrated by E-W cross-section of the study area (Cross-section A-A is indicated by white line in Figure 2.4)

The thrust contact indicated by red arrow (Figure 2.5) dip at 30^0-40^0 towards W and NW and characterized by intense deformation. The mafic-ultramafic constitute the hanging wall of the thrust surface and are schistose with intensity of deformation and grade of metamorphism decreasing away from the thrust surface. The intensity of mineral lineation and tectonic foliation also decreases away from the thrust surface.

Intensive alteration in the shear zones is apparent. The alteration is thought to be as a result of fluid movement which is considered responsible for mineralization or re-concentration of the gold. Four types of alteration zones exist in the area, carbonatization, feldsphatization, tourmalinization and sericitization. Zonings of alteration in typical magmatic hydrothermal alteration are common features of Okote granodiorite mineralization.

The Okote gold mineralization is an example of such an extremely complicated system including, with at least two styles of gold mineralization including vein type and granodiorite hosted disseminated types. Metagranodiorite mineralization is characterized by disseminated sulphides. The sulphides are undeformed and not aligned both down dip and along strike instead they are randomly dispersed in the rock unit.

There are also gold mineralizations hosted in narrow shear zones. Veining and therefore mineralization is discontinuous with this type of hydrothermal deposit. This kind of mineralization is hosted within a relatively narrow shear zone or zones, which cross cut the trend of the dominant foliation and relict lithological contacts. The narrow shear zones strike at 008-012° while the dominant foliation and relict lithological contacts at 020°, both dipping to the west at high angle (Figure2.6).

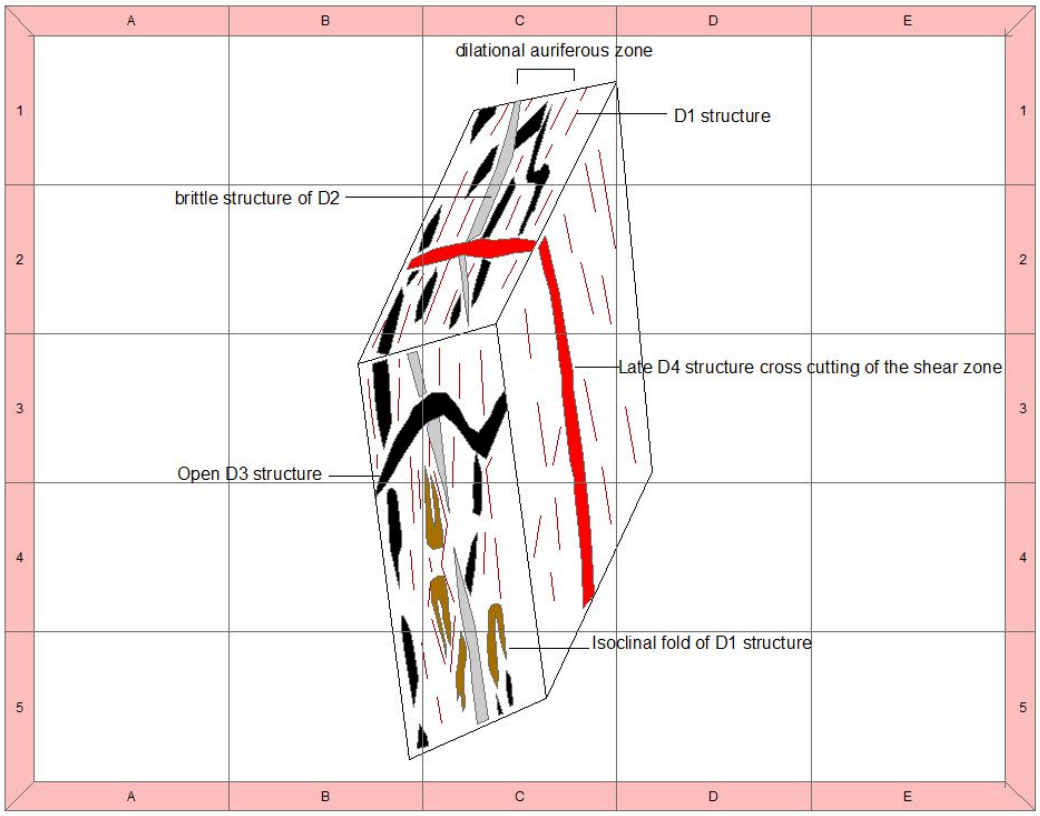

Figure2.6. Schematic model showing deformational events of Okote (D1, D2, D3 and D4) with their cross-cutting relationships

The past exploration activity undertaken by NMiC, Dawa Digati gold exploration areas have identified 5 major gold prospects (Ginchile, Burikaro, Ejersa South, Dhugo sefer and Okote) along strike with Okote area during the first phase exploration period. Out of these the Okote gold prospect was found to be strongly mineralized and called for follow-up as it produced further exploration with respect to gold contents up to 40g/t gold was locally discovered in quartz vein hosted in carbonate chlorite schist.

Currently mineral resource estimate was completed for the Okote deposit according to the guidelines

set out in the Canadian Code for reporting of Exploration Results by Mineral Resources and Mineral Reserves, NI43-101 (an Independent consulting firm Venmyn rand, pty). According to the report, the Okote Project is low grade and high tonnage gold deposit (A.Clay, 2012).

The shear zone hosted, mesothermal, gold mineralization also occurs in the Okote area along three N-S striking ductile shear zones, with different intensity of shearing and hydrothermal alteration which cut the mafic rocks. These shear zones reveal zonings from slightly altered but not sheared protolith at shear boundaries followed by transitional zone up to mylonite zones at the center. Auriferous quartz-carbonate-tourmaline veins occur mainly in the mylonite zone. Combining structural and spatial association of gold with greenschist facies, the mineral and wall rock chemistry, fluid inclusion data, together with isotopic data concluded that the Okote gold mineralization formed by interaction of structurally controlled hydrothermal fluids with mafic rocks (Debele and Koeberl;2004). Two phases of mineralization are recognized by a subsequent work. These include the gold-sulphide-quartz and sulphide-carbonate-quartz mineralizations. Visible gold particles are commonly encountered in boxwork association of fractured and limonitized pyrite structure. The mineralization is controlled by shearing, with pinch and swell structures both along the strike and down the dip. The association of gold with sulphides in the quartz veins at Okote was taken as the evidence of gold transport as bisulphide complex (Abu Wube, 2005). A primary "porphyry type" metagranodiorite hosted gold deposition is latter identified in the study area. The gold is thoroughly hosted by metagranodiorite and quartz veins in it. This was interpreted as mineralization by saline metal scavenging chloride complex as responsible fluid that leaches out metal (Au) from the silicate melt of magma during its accent to near surface depositional site and later dropped the metal in the pore spaces and voids of the porphyritic textured acidic intrusive (Solomon, 2015), similar to Digati type primary biotite gneiss hosted milky white quartz vein with fluid inclusion data suggesting Au-transport by Cl-complex (Aster etal.1988b as cited in Schmerold,1989).

2.2. Research gap

Except the porphyry type magmatic hydrothermal fluid suggested by Solomon (2015) and the saline hydrothermal fluid by Hamrla (1977) that showed some clues about alternate models for gold mineralization in southern Ethiopia, other researchers majorly focused on structurally controlled shear zone hosted mesothermal lode gold mineralization (Debele and Koeberl;2004).

Wayu Boda gold project is located in the mineral rich central-southern Adola greenstone belt in southern Ethiopia, exactly 24km south of Okote prospect. Geological mapping of trenches indicates that the main potential of gold mineralization may be proximal to granite/schist contacts mainly hosted by the granitoid unit (Alecto minerals, 2013).

The presence of granitoid hosted Malachite and Azurite with erratic, scattered, positive & localized value of copper mineralization in Gewale, Wachile and Horoto (south of Okote) might need geological attention and professional discussion to its ore genesis to come out with final conclusion about the copper project (Kenea etal; 2003). Most recently, local artisanal miners are mining copper in these prospects following exposure of green malachite by trenches (Figure 2.7). The occurrence of copper and the presence of mineralized granodiorite in the area is interesting. It may indicate the presence of porphyry type deposit at the vicinity as outlined by Solomon (2015).

Analytical results of auriferous quartz veins from metatonalite of Dawa-Digati Meissa prospect contain considerable Cu and Pb. Exploration work by JCI and MIDROC companies discovered low grade and high tonnage granodiorite hosted gold deposition in a specific locality called Werseti of Adola greenstone belt.

In light of these occurrences, further research is required to elaborate the role of intrusion in gold mineralization, and presence/absence of intrusion related gold deposits in the region. This research is therefore will be directed to understand the role of intrusion in orogenic polypase gold mineralization of southern Ethiopia.

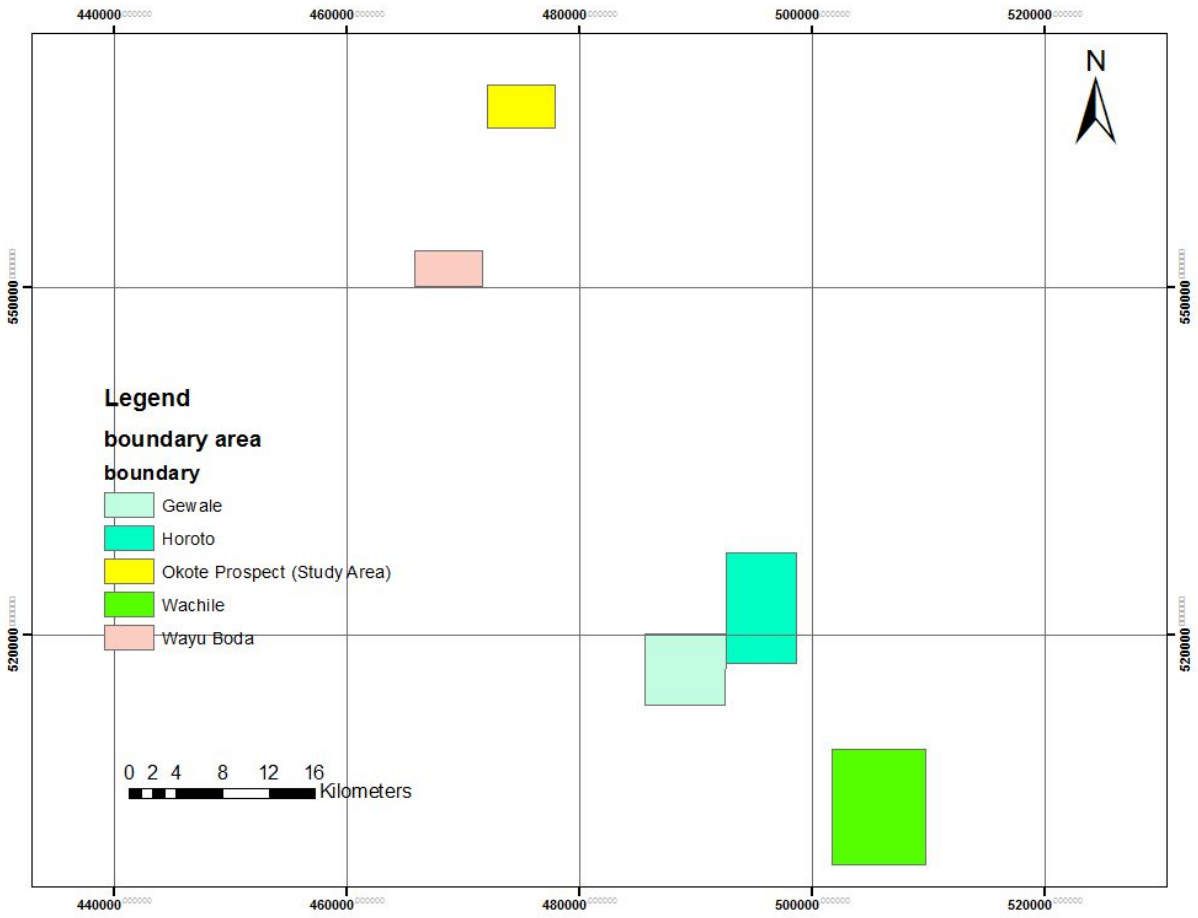

Figure2.7. Spatial distribution of intrusive related gold and copper occurrences; Okote, Wayu Boda, Horoto, Gewale and Wachile

2.3. Research questions

In order to understand the role of granitoid in gold mineralization, the research is planning to address the following questions:-

1. Verification of the generation of mineralization (shear zone hosted Vs granitoid hosted)
2. What is the chemistry and trace elements signature of mineralizing fluid?
3. What is the temperature of formation for the fluid?
4. What is the process and source of granodiorite hosted gold mineralization?
5. What is the link between the shear zone hosted, vein type and granitoid hosted disseminated gold mineralization

2.4. Research objective

2.4.1. General objective

As it stands based on the available data, it can be hypothesized that Okote gold deposit may represent the superposition of two hydrothermal events, one related to intrusive and the second to remobilization by ‘‘orogenic-style” hydrothermal fluids. Genetically, it may be suggested that early ore fluids were derived from a deep- seated source involving magmatic-hydrothermal processes followed by a structural overprint and associated remobilization of gold.

One of the keys to better understand the formation of the deposit is the timing of the high grade mineralization relative to the deformation, metamorphism, and hydrothermal activity. This is one of the outstanding problems in the understanding of the formation of orogenic gold deposits. The interpretation of the age of gold mineralization in the Okote district has evolved from largely syn-tectonic to pre-regional deformation and metamorphism and associated with strike slip faulting by previous workers. Two stages of mineralizations were proposed, with the main stage corresponding to D2 and a subsequent D3 but lesser event, represented by auriferous quartz-pyrite-tourmaline vein, carbonate-chlorite schist.

Greenstone hosted gold deposits are typically products of complex hydrothermal systems that evolved multiple fluids at various times throughout their histories. The Okote gold mine area is an example of such an extremely complicated system including, with at least two styles of gold mineralization (Solomon, 2015).

1- Intrusive related gold mineralization hosted by granodiorite
2- Shear hosted gold mineralization

Therefore, the major objective of this research is to study and understand the role of granodioritic intrusion in the polyphase gold mineralization of Okote area.

2.4.2. Specific objectives

Details of the research objective are as follows;

i. Detail and systematic sampling of the alteration zones, the quartz veins and host rock for microstructure studies, metamorphism studies, isotopic and fluid inclusion studies. The sampling focused on the main research area, Okote, but it was also conducted from the areas along strike (Wayu-Boda, Gewale, Wachile, Horoto and prospects) for comparison and required understanding.

ii. Determination of source rock and tectonic setting by major elements oxide determination using XRF and trace elements geochemistry using ICP-MS

iii. Determination of temperature of deposition by decrepitation using barometry

iv. Determination of FI type using petrographical study

2.5. Research method

Geological mapping, structural analysis and sampling are the main field methods of the research. Representative field and drill core samples are taken from all sites of granodiorite distributed both across and along strike of the intrusive with varying depth. Detail surface geological studies and re-logging of drillholes and trenches were the main methods adopted to characterize the mineralization and alteration associated with metagranodiorite. GARMIN 72H model GPS instrument is used to navigate across the prospect area and capture spatial data where necessary. Geological hammer, HCL acid, pencil magnet and hand lens with 10X magnification are also used to facilitate the proposed research work. Geological structures such as foliation, lineation, faults, shear zones and folds are measured using Brunton compass.

Fluid inclusion, trace element geochemistry using ICP-MS and major element oxide by XRF are the major analytical methods adopted to accomplish the research objective.

i. Litho-geochemical study by whole rock analysis using XRF and ICP_MS methods is an important tool for understanding ore-forming geological process and environment. Eight samples for major elements oxide by XRF and twenty samples for multi-elements determination using ICP-MS are analyzed at ALS global analytical laboratory located at

Ireland.

ii. Fluid inclusion petrography and analysis by baro-acoustic method for the determination of temperature of deposition by heating to decrepitation and determination of CO_2 content is applied for characterization of mineralizing fluid responsible to Au & Cu deposition at the prospect areas. The growth of grains is never perfect, samples of fluid in which the crystals grew may be trapped in tiny cavities usually <100 micro meter in size deciphering the formational history of many rock types particularly valuable in developing our understanding of ore genesis especially in the subject of ore transport and deposition. Understanding the fluid inclusion of quartz mineral of granodiorite clarifies the type of fluid responsible for the genesis of gold related to the intrusive. Fifteen samples are analyzed at Burlinson geochemical laboratory for fluid inclusion study using baro-acoustic decrepitation method. FI petrographical study is also performed at Burlinson geochemical laboratory located in Australia.

CHAPTER THREE

3. GEOLOGY

3.1. Regional geology and tectonics

The presence of ophiolite complexes in NE and E Africa has been documented using Landsat, field and geochemical studies. Five major ophiolitic sutures are identified in NE Africa, while plate reconstruction of Africa and Madagascar suggests a possible sixth ophiolite belt to the east. The ophiolites are considered to be remnants of supra-subduction zones and back-arc basins. The ophiolites are dismembered, and their mode of occurrence varies widely resulting in different structural relationships. In Western Ethiopia, the Yubdo complex is formed of harzburgite which grades into a cumulate sequence of ultramafic and gabbroic rocks and metabasalts, while data from the Adola-Moyale belt **(S.** Ethiopia-NE Kenya) indicate an island-arc and MORB geochemistry, which developed in a back-arc tectonic setting. Regional geological, tectonic and geochemical studies suggest rifting at ***c.*** 1200Ma and subsequent convergence led to the development of intraoceanic arcs and associated marginal basins in the north and narrow basins within the sialic basement gneisses further south in Kenya and Tanzania. This was followed by continent-continent collision which led to accretion of island arcs by gentle collision from the northeast in Saudi Arabia and severe crustal shortening in **S** Sudan, Kenya and SE Ethiopia as compared to Saudi Arabia, NE Sudan and N and W Ethiopia owing to oblique collision from the southeast (Sife M. Berhe, 1990). The four Neoproterozoic ophiolitic belts in southern Ethiopia mentioned by Berhe (1990) is latter on confirmed by (B.Yibas., W.U.Reimold., C.R.Anhaessser. and C.Koeberl., 2002) —Megado, Kenticha, Moyale-El Kur and Bulbul.

In Adola, southern Ethiopia, mafic and ultramafic igneous rocks occur in narrow, 4-10 km wide, north-south trending belts bounded by high-grade gneisses and migmatites. The mafic/ultramafic rocks are complexly deformed and metamorphosed in greenschist to lower amphibolite facies and are thought to be tectonically dismembered parts of an ophiolite complex (Begashaw W., Zemen A., Zerihun D.and Julio J.G.; 1996). This is in good agreement with (B. Yibas, 2002); two distinct tectonostratigraphic terranes, separated by repeatedly reactivated deformation zones, are recognized in the Precambrian of southern Ethiopia: (1) granite-gneiss terrane, which is classified into sub-terranes and complexes, and (2) ophiolitic fold and thrust belts. The granitoid gneisses form an integral part of the granite-gneiss terrane, but are rare in the ophiolitic fold and thrust belts. The

ophiolitic fold and thrust belts are composed of mafic, ultramafic and metasedimentary rocks in various proportions. Okote is situated in Megado ophiolitic fold and thrust belt of southern Ethiopia.

3.2. Local geology

Okote prospect area is thoroughly covered by felsic and mafic metavolcanics often mylonitized at their contacts. Metagranodiorite and aplitic dykes are the felsc rocks while metagabbro, amphibolite, metadiorite, chlorite-amphibole schist, chlorite schist and talc schist are the intermediate-mafic-ultramafic sequences outcropped on the prospect. Four generations of quartz veins are hosted by the metavolcanics indicating the various episodes of the locality. The felsic rocks are repeatedly observed intruding the mafic rocks. The metavolcanics of the study area exhibit sharp contacts, except metagabbro-amphibolites gradational contact which are mapped as one unit. Mafic xenoliths hosted by granodiorite are common features of the contact area while lenses of granitoids are widespread in the protholith. The contact of the two metavolcanics is marked by mylonitization which is a common feature at this zone.

Comprehensive geological and genetic model can be reached after, detail discussion of the mappable rock formations on the major lithologies of Okote prospect area. Forty four thin sections from the project archive and eight x-ray fluorescence analysis primary data are used to outline petrograhic description, whole rock analysis and lithogeochemistry of the prospect.

Metagranodiorite and aplitic dyke are the only two genetically related felsic rocks of the study area. Mineralogically the two units resemble each other except that opaque minerals emerge on metagranodiorite unit which shows its mineralization. They have distinct textural difference with the latter one is fine grained and appear as dyke. Metadiorite, Metagabbro, Amphibolite, Chlorite-Amphibole schist, Chlorite/Carbonate-Chlorite schist and Talc schist are the intermediate-mafic-ultramafic sequences exposed on the prospect.

Apilitic dyke is a light gray color and fine to medium grain schistose textured granite. This dykes or small stocks commonly intrude the mafic metavolcanics of the prospect.

The whitish and soapy textured ultramafic, Talc schists is scarcely noticed in north Okote. However most of them are thin and lenticular. They are usually discontinuous along strike and occur as patches here and there hosted by the shear zone. These rocks are usually schistose but sometimes grade to massive varieties in central Okote. Euhedral pyrite and magenetite crystals are observed at several places, particularly in the tremolite-actinolite-talc schist.

The intensive shearing and deformation revealed the invasion of the locality by various generations of quartz veins. Four main types of quartz veins are known in Okote prospect. The first three are concordant and while the last one is discordant to the regional foliation. The east-west running discordant quartz vein is characterized by glassy to milky white appearance, massive textured and barren with respect to gold. This might indicate that the E-W discordant quartz vein originated by a post deformational event cross-cutting the earlier mineralization. The concordant glassy white colored quartz vein trends towards NNW-SSE to NNE-SSW along the shear zone which is characterized by sulphidation and tourmalinization. The gold mineralization is megascopically visible. The metagranodiorite rock unit is intensely invaded by quartz vein. The contact of metagranodiorite is characterized by mineralized quartz veins and stringers.

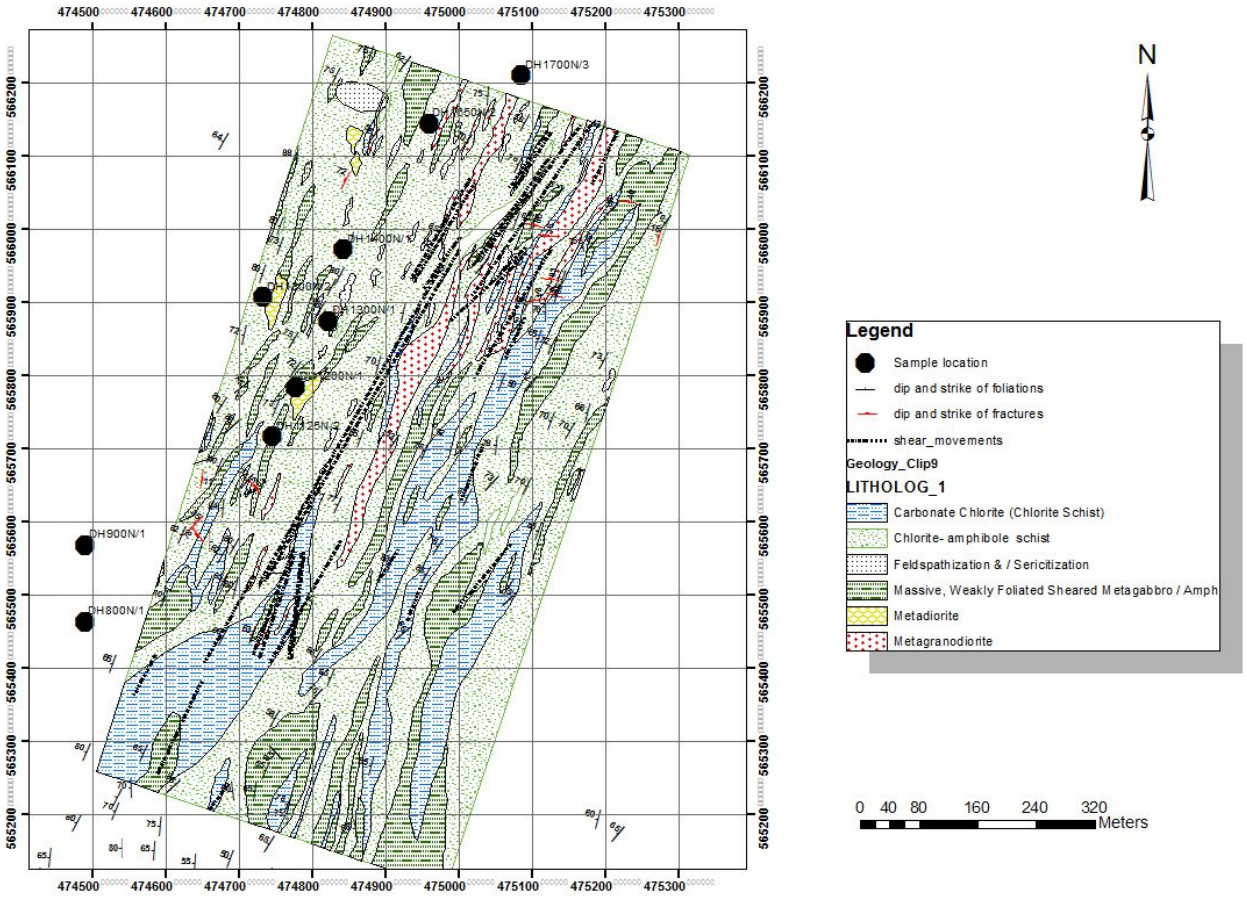

Figure3.1. Geological map of study area; UTM projection, Adindan datum, zone 37N coordinate system is used; **National Mining Corporation (2010)**

3.2.1. Metagranodiorite

It is a dark gray rock with laths of pale greenish tint colored and fine to medium grained and schistose felsic intrusive. Textural study of metagranodiorite showed the rock acquires porphyritic texture with coarse grained feldspar phenocrysts placed on finer grained ground mass. The schistocity is marked by a faint segregation of muscovite mica from that of quartz and feldspar. Two penetrative foliations dipping at $65^0$and 40^0 towards 340 and 110 have been observed in the prospect where the metagranodiorite is exposed. The modal percentage of the rock composition is 35% quartz, 15% muscovite, 13% chlorite, 10% biotite, 12% calcite, 10% plagioclase and 5% opaque minerals. The texture varies from xenoblastic to hypidio-xenoblastic quartz and calcite with tiny-platy micas and chlorite. Quartz, chlorite, biotite and muscovite show well developed parallel alignment of schistosity. Plagioclase altered to calcite and biotite is replaced by chlorite. The granodiorite of Wayu-Boda and Horoto are characterized by intense mineralization of secondary copper minerals like malachite and azurite (Plate 3.1).

Plate3.1. Horoto prospect granodiorite showing Malachite and Azurite mineralization (not to scale)

Metagranodiorite and aplitic dyke are the only two genetically related felsic rocks of the study area. Mineralogically the two units resemble each other except that opaque minerals emerge on metagranodiorite unit which shows its mineralization. They have distinct textural difference with

the latter one appearing as dyke. This dykes or small stocks commonly intrude the mafic metavolcanics of the prospect. The aplitic dyke is normally exposed for 1-2m width and hence too small for mapping and not considering as a major petrographic unit.

3.2.2. Metadiorite

It is a pale greenish gray colored sheared rock with medium grain and relict texture. The modal percentage of the rock composition is 30% epidote, 20% plagioclase, 20% hornblende, 15% quartz, 10% chlorite and 5% opaque minerals. Most of the mafic minerals exhibit xenoblastic texture with relicts of plagioclase and platy chlorite. Hornblende is partially and completely replaced by chlorite and epidote. Re-crystallization of quartz and plagioclase is seen in the matrix. Plagioclase is altered to epidote. Hornblende and chlorite show weak sub parallel alignment. Patches of quartz veins are also peculiar feature of this rock unit.

3.2.3 Metagabbro

It is a gray and pale greenish tint colored sheared mafic rock with medium to coarse grained texture with anatomizing schistocity. The modal percentage of the rock composition is 30% hornblende, 25% plagioclase, 20% epidote, 10% chlorite, 10% quartz, 5% opaque minerals with trace of apatite. The texture of the rock is characterized by relict of plagioclase with platy chlorite embedded on xenoblastic quartz and mafic mineral. Hornblende and chlorite are epidotized and re-crystallization of quartz and plagioclase is seen in the matrix. Plagioclase altered to epidote. Hornblende and chlorite show weak sub parallel alignment.

3.2.4. Amphibolite

It is a light to dark gray colored, fine to medium grained texture with faint schistocity. The modal percentage of the rock composition mainly composed of 50% actinolitic-hornblend, 20% epidote, 17% chlorite, 12% plagioclase and 1% opaque (Fe-oxide/magnetite). The mafic minerals have xenoblastic texture with platy chlorite and relict of plagioclase. The relict plagioclase is completely altered to epidote. Actinolitic-hornblende replaced by chlorite. Veins of epidote and plagioclase are seen along the section. Actinolitic-hornblende and chlorite show well developed parallel alignment. In most case the unit is intensely magnetiferous. It usually

exhibits gradational contact with metagabbro, with slight differentiation in texture and abundance of plagioclase.

3.2.5. Chlorite-Amphibole Schist

It is pale greenish gray in color with medium to fine grain and schistose textured mafic rock unit. It is the most abundant rock formation of the study area. The modal percentage of the rock composition is 35% epidote, 20% hornblende, 15% quartz, 10% chlorite, 15% plagioclase and 5% opaque minerals. Idio-Xenoblastic quartz and mafic minerals with platy chlorite and relict plagioclase define the texture of the rock. Chlorite and hornblende shows well developed parallel to sub parallel alignment of schistosity. Hornblende is replaced by chlorite and epidote. Plagioclase is altered to epidote. Re-crystallization of quartz and plagioclase is seen in the section.

3.2.6. Chlorite Schist/Carbonate-Chlorite Schist

It is dark gray in color, fine to medium grain schistose textured mineralized mafic rock. The unit is intensely foliated. The quartz veins with a pinch and swell structure are concordant with the foliation. It contains auriferous quartz carbonate tourmaline veins. Rhombic, euhedral crystals of pyrite is the distinguishing feature of the unit. Gold grains accompany the crystals of pyrite. It is highly carbonatized. The modal percentage of the rock composition is 35% chlorite, 30% calcite, 20% quartz, 7% plagioclase, 5% biotite and 3% opaque minerals. Matrix is mainly composed of calcite, chlorite and quartz exhibiting parallel alignment. Plagioclase is altered to calcite and biotite is replaced by chlorite.

CHAPTER FOUR

4. STRUCTURE, METAMORPHISM AND STRATIGAPHY

4.1. Structure

Adola gold belt has undergone polyphase deformation which has resulted in the development of N-S ophiolite suture zones. Both the greenstone and gneissic terrains have been affected by N-S trending faults of regional to local significance. The structural features of Adola gold field are attributed to 3 episodes of deformation, though this has not been commonly adopted (Worku and Schandelmeier, 1996).

The Okote gold field had undergone a polyphase deformation which resulted in the existing planar features (foliation, axial plane cleavage and fault) and linear features (mineral lineation, boudins, striations). The regional penetrative foliation generally trends N20E. Both Legadembi and Okote lie on the same shear zone called "Legadembi-Aflata".

Remote sensing, detail dip and strike measurement from secondary data and field measurements have been tried to be analyzed to outline and reach into identification of structural controls of mineralization of the study area (see Figure 4.1).

Detail structural study was conducted in the study area focusing on structures which are more related to porphyry mineralization. Primary data collections by measuring dip and strike of foliation and plunge of fold are the only method adopted to accomplish the purpose.

Field observations and measurements indicate several strong periods of polyphase folding. The rocks of Okote area underwent the effects of polyphase deformation with at least 3 deformation events affecting the region D1, D2 & D3 (Worku and Schandelmeier, 1996). The most prominent planar feature is shear foliation of country rock, which generally strikes 018-198 (NNE-SSW) and dip to the west at high angle. The N-S trending shear zones have anatomizing pattern with intervening lenses of less deformed mafic rocks and dip moderately to steeply towards west.

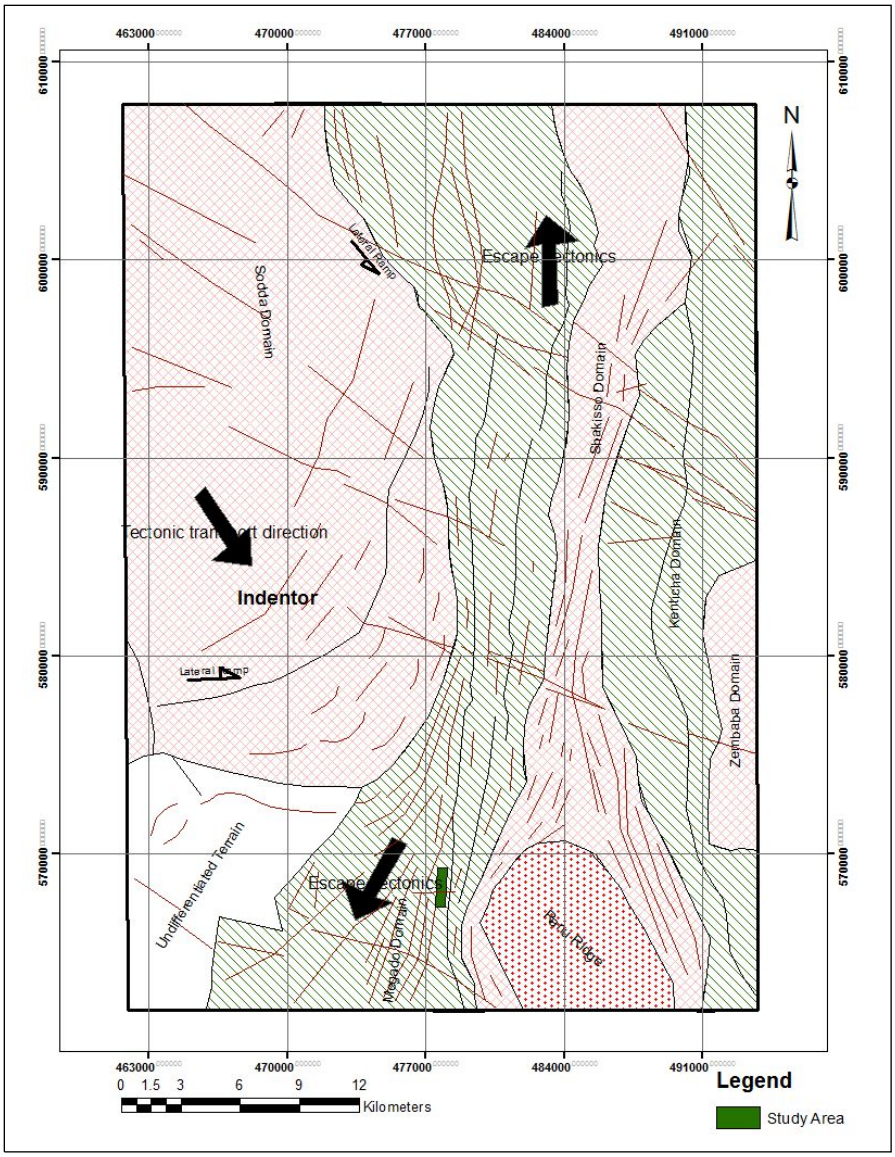

Figure4.1. Major syn-tectonic granite and shear zone development of Adola region with domains and greenstone belts (from sat. Image after Worku H. & Schandelmeier 1996)

Two penetrative foliations dipping at $65^0$and 40^0 towards 340 (W) and 110 (E) have been observed in the prospect where the metagranodiorite is exposed. This may represent stokes of porphyries projecting from the main body dipping at different direction which is a characteristics of transpression at accretion zone. Rose diagram plots of fracture show 098-278 mean resultant direction by indicating an east-west running fracture zone (D4) which is latter filled by milky white barren quartz vein discordant to the relict of lithology, which is also shown in Figure 2.4

indicated by red arrow. The structural control in favor of gold mineralization is the shear foliation striking 018-198 and dipping towards west at high angle (65-70^0). This narrow shear zone coincides with the shear hosted mesothermal lode carbonate-chlorite hosted gold mineralization rather than the porphyry type granodiorite hosted gold mineralization, which shows its disobedience to the main shear zone.

Plate4.1. Relict of lithology 020 (D1) over printed by shear zone 008 (late D2 & D3)

A narrow shear zone cross-cuts the relict of the lithology at an acute angle. The shear zone and foliation strike at 008-012° and 020°, both dip to the west. The quartz stringer and buckled quartz vein justify the cross cutting relationship of the shear zone and relict of lithology.

4.2. Metamorphism

Adola area poly metamorphic history of the units can be subdivided in to at least three events. M1 is the earliest event and seems to be restricted to all the basements. M2a and M2b affect all units and are separated from M1 by a period of uplift and erosion. M2a and M2b are also clearly separated by a time gap, but they seem to belong to the same metamorphic-deformational cycle. M2a is the most pronounced metamorphic event which has produced the dominant metamorphic mineral assemblages in the area. M2b is a late, mostly post deformational (post folding phases),

event of retrograde overprinting. Due to the intensity of M2a, almost no relict features of the M1 event are preserved. The only evidence for M1 is fragments of basement rocks (amphibolite, quartz-K-feldspar gneiss, biotite schist, biotite gneiss) in the metamorphosed (by M2a/b) and deformed (folding phases) metaconglomerates and metasandstones. In addition garnet relicts in amphibolte of the western gneiss might also belong to the M1 event (Schmerold etal.; 1988).

The region is generally characterized by lower amphibolite to upper greenschist facies metamorphism of the meta-volcano-sedimentary assemblages. Lower grade metamorphism has subsequently affected some of the units. A few regional petrography studies show that the following mineral assemblage in volcano-sedimentary rocks: muscovite, biotite, quartz, sodic plagioclase in the metasediments and hornblende, biotite, quartz, sodic plagioclase, epidote in the metavolcanics. Mineral assemblages, especially the abundance of muscovites and sodic plagioclases even in the mafic rocks (volcano-sedimentary rocks) is typical of lower amphibolite facies metamorphism. Some meta-volcano-sedimentary assemblages also contain chlorites and sericites, which might be, related either, to original greenschist facies metamorphism at the subduction fronts or, to later retrograde low-grade metamorphism. Both are possible as some of the rocks contain chlorites and epidotes as the dominant metamorphic minerals while in other cases sericites and epidotes occur around altered feldspars, and chlorites surrounding altered hornblende. This is in agreement with regional studies (e.g., Asrat et al., 2001; Ayalew et al., 1990; as cited in Solomon, 2015).

Both the gneissic and greenstone rocks of the Adola have been subjected to variable intensities of greenschist-amphibolite facies of metamorphism. The megado greenstone rocks generally exhibit effects of low grade green schist facies metamorphism. Lithologies of the study area show metamorphic textures, such as foliation, lineation and bandings produced by regional metamorphism and shearing.

Grade of metamorphism increases while moving to the east of Okote towards Ranu ridge of the central high grade gneissic terrain, the metamorphism is disrupted by north-south trending shear zone. The mafic-ultramafic constitute the hanging wall of the thrust surface and are schistose with intensity of metamorphism decrease away from the thrust surface (see Figure 2.4).

Numbers of lithologic units are exposed in Okote, metamorphic features of granodiorite unit have been discussed here for the purpose of satisfying the main objective of the research.

Transmitted light microscopic analysis of thin section showed that quartz, chlorite, biotite and muscovite developed parallel alignment of schistosity. Microscopical observation revealed that the rock unit here under discussion developed limited deformational fabrics. The original igneous texture and mineralogy are recognisable and yet preserved by suggesting lower grade metamorphism.The mineralogical assemblage muscovite, biotite, chlorite, calcite, plagioclase and quartz indicate low grade metamorphism of greenschist facies. The transition from greenschist facies to amphibolite facies is indistinct in most areas but is marked by the breakdown of actinolite to hornblende. The presence of actinolitic hornblende in one of the analyzed granodiorite rock unit tells us the entrance to amphibolite facies. Lithologies derived from low-grade metamorphism of the metavolvanic of the prospect, consist largely of chlorite, actinolite, calcite, plagioclase and quartz. This is a characteristic feature of upper greenschist and lower amphibolites facies metamorphism (Barker, 1998).

Table 4.1.Schematic paragenetic sequence of the study area

D1	**D2**	**D3**	**D4**
Low angle thrust fold (Nappe)	High angle thrust fold	Sinistral strike slip shearing	Fracture zone (E-W)
M2a	M2b	M2b	-
Qv1	Qv2	Qv3	Qv4
Silicification and Suplidation (needle like Pyrite)	Potassic, Argilic, Phylic alterations and disseminated sulphides (Pyrite & Pyrrhotite and minor Chalcopyrite)	Carbonatization, Sericitization, Tourmalinization and rhombic Pyrites	Not altered
Not mineralized	Granodiorite hosted porphyry type Au & Cu mineralization	Carbonate-chlorite & shear hosted lode Au mineralization	Barren milky white quartz
N20^{0}E (Regional foliation)	**N008^{0}E (Shear zone @ late D2 & D3)**		**E-W (Fracture zone @ D4)**

4.3. Stratigraphy

Okote prospect area is located in southern Ethiopia at the southern extension of the Adola gold belt. The geology of Okote prospect is part of the southern extension of the metavolcano-sedimentary rocks of the Adola belt lying in Megado lithostructural domain.

About 2 km east of the prospect area, one can see the Burjiji–Gariboro gneiss (Ranu granitic gneiss), while the western side of the prospect is characterized by intercalation of metagranodiorite and amphibolite. The Burjiji-Gariboro gneiss marking the eastern contact of the Megado-Volcano Sedimentary belt is a prominent unit that stretches almost throughout the length of the belt. Lithologically, the area is comprised of schists mainly chlorite- amphibole, carbonate-chlorite, talc-tremolite and associated intrusive ranging from granodiorite to metagabbro of different compositions.

Litholohgical and structural evidences observed during the field exploration works of the prospect outlined that biotite-quartzofeldspathic gneiss and amphibole-quartzofeldspathic gneiss represent the lowest stratigraphic units by showing a tectonic contact with the overlying mafic-ultramafic rocks (meta-ultramafic rocks, amphibolite, metagabro, and other meta-volcanics) and which are latter intruded by intermediate to felsic /syn/post tectonic intrusion (granodiorite).

CHAPTER FIVE

5. GEOCHEMISTRY

Geochemical analysis of rocks using inductively coupled plasma mass spectrometry and x-ray fluorescence was carried out to outline the whole rock chemistry, source rock, magma type and tectonic setting of the study area.

Inductively coupled plasma mass spectrometry or ICP-MS is an analytical technique used for elemental determinations. The technique was commercially introduced in 1983 and has gained general acceptance in many types of laboratories. Geochemical analysis labs were early adopters of ICP-MS technology because of its superior detection capabilities, particularly for the rare-earth elements (REEs). ICP-MS has many advantages over other elemental analysis techniques such as atomic absorption and optical emission spectrometry, including ICP Atomic Emission Spectroscopy (ICP-AES). An ICP-MS combines a high-temperature ICP (Inductively Coupled Plasma) source with a mass spectrometer. The ICP source converts the atoms of the elements in the sample to ions. These ions are then separated and detected by the mass spectrometer.

XRF (X-ray fluorescence) is a non-destructive analytical technique used to determine the elemental composition of materials. XRF analyzers determine the chemistry of a sample by measuring the fluorescent (or secondary) X-ray emitted from a sample when it is excited by a primary X-ray source. Each of the elements present in a sample produces a set of characteristic fluorescent X-rays ("a fingerprint") that is unique for that specific element, which is why XRF spectroscopy is an excellent technology for qualitative and quantitative analysis of material composition.

Twenty eight core samples from selected drill holes were collected for geochemical analysis using inductively coupled plasma mass spectrometry and X-ray Flourescence analytical methods. Rare earth elements (REE's) and many other trace elements including Sc, Cr, Rb, Sr, Zr, Ba, Hf, Ta, Th, and U were analyzed by ICP-MS methods while whole rock analysis by fusion to study the major elements oxides abundance is performed by XRF method. The chemical analysis is performed in the internationally accredited ALS global commercial laboratory located in Ireland. The samples are representative and collected randomly both along strike and across the depth of the lithologies from north Okote prospect area.

Table5.1. Samples for geochemical analysis with desurveyed spatial data from Datamine software

#	Method of analysis	Lithology	Sample Code	Location			Remark
				X	Y	Z	
1	XRF (Major elements)	Chlorite-Amphibole schist	CAS-XRF-01	0474778	0566005	1399	DH1400N/1; core sample
2	XRF(Major elements)	Carbonate-Chlorite schist	CCS-XRF-02	0474564	0565375	1155	DH800N/1 ; core sample
3	XRF(Major elements)	Metagabbro	MG-XRF-03	0474512	0565507	1314	DH900N/1 ; core sample
4	XRF(Major elements)	Amphibolite	A-XRF-04	0474828	0585870	1412	DH1300N/1; core sample
5	XRF(Major elements)	Metadiorite	MD-XRF-05	0474856	0565694	1252	DH1200N/1; core sample
6	XRF(Major elements)	Metagranodiorite	MGD-XRF-06	0474981	0566189	1502	DH1650N/2 ; core sample
7	XRF(Major elements)	Metagranodiorite	MGD-XRF-07	0474799	0565717	1362	DH1200N/1 ; core sample
8	XRF(Major elements)	Metagranodiorite	MGD-XRF-08	0474789	0566001	1374	DH1400N/1 ; core sample
9	ICP_MS (Trace elements)	Chlorite-Amphibole schist	CAS-ICP-01	0474552	0565491	1223	DH900N/1 ; core sample
10	ICP_MS (Trace elements)	Carbonate-Chlorite schist	CCS-ICP-02	0474550	0565492	1227	DH900N/1 ; core sample
11	ICP_MS (Trace elements)	Metagabbro	MG-ICP-03	0474827	0565870	1414	DH1300N/1; core sample
12	ICP_MS (Trace elements)	Amphibolite	A-ICP-04	0474512	0565399	1261	DH800N/1 ; core sample
13	ICP_MS (Trace elements)	Metadiorite	MD-ICP-05	0474839	0565700	1287	DH1200N/1; core sample
14	ICP_MS (Trace elements)	Metagranodiorite	MGD-ICP-06	0475005	0566180	1447	DH1650N/2 ; core sample
15	ICP_MS (Trace elements)	Metagranodiorite	MGD-ICP-07	0474782	0565852	1349	DH1300N/2; core sample
16	ICP_MS (Trace elements)	Metagranodiorite	MGD-ICP-08	0474816	0565643	1233	DH1125N/2; core sample
17	ICP_MS (Trace elements)	Metagranodiorite	MGD-ICP-09	0474611	0565463	1103	DH900N/1 ; core sample
18	ICP_MS (Trace elements)	Quarz vein	QV-ICP-10	0474848	0565631	1173	DH1125N/2; core sample
19	ICP_MS (Trace elements)	Metagranodiorite	MGDGC-01	0474704	0565640	1307	BH1100N/1; core sample
20	ICP_MS (Trace elements)	Chlorite_Amphibole schist	CASGC-04	0474761	0565620	1179	BH1100N/1; core sample
21	ICP_MS (Trace elements)	Quartz Vein	QVGC-05	0474688	0565646	1344	BH1100N/1; core sample
22	ICP_MS (Trace elements)	Metagranodiorite	MGDGC-06	0474900	0565853	1250	BH1350N/1 ; core sample
23	ICP_MS (Trace elements)	Metagabbro	MGGC-07	0474893	0565855	1262	BH1350N/1 ; core sample
24	ICP_MS (Trace elements)	Metagranodiorite	MGDGC-08	0474933	0566044	1457	BH1550N/1 ; core sample
25	ICP_MS (Trace elements)	Metagranodiorite	MGDGC-11	0475045	0566162	1462	BH1700N/1 ; core sample
26	ICP_MS (Trace elements)	Quartz Vein	QVGC-12	0475180	0566058	-	TR231; channel sample
27	ICP_MS (Trace elements)	Aplitic dyke	APGC-13	0475111	0566003	1466	Chip sample near to BH1550N/2
28	ICP_MS (Trace elements)	Carbonate-Chlorite schist	CSGC-14	0475115	0566005	1467	Chip sample near to BH1550N/2

Table5.2. Whole rock analysis using x-ray fluoresce method for major and minor elements oxides

Sample codes	CAS-XRF-01	CCS-XRF-02	MG-XRF-03	A-XRF-04	MD-XRF-05	MGD-XRF-06	MGD-XRF-07	MGD-XRF-08
Al2O3	13.74	16.04	20.23	15.14	12.58	14.99	12.18	13.63
BaO	0.04	0.07	0.04	0.06	0.02	0.04	0.01	0.04
CaO	11.7	10.7	9.42	7.23	3.4	5.55	3.25	1.74
Cr2O3	0.09	0.01	0.01	0.05	<0.01	<0.01	<0.01	<0.01
Fe2O3	9.46	8.36	9.23	7.87	3.58	6.52	4.62	3.61
K2O	1.14	0.83	1.14	0.92	0.4	0.69	0.09	2.03
MgO	8.08	6.87	6.52	7.54	0.64	1.49	0.64	0.33
MnO	0.18	0.16	0.15	0.13	0.09	0.14	0.12	0.04
Na2O	1.4	2.3	3.47	3.77	3.78	3.41	3.8	2
P2O5	0.24	0.04	0.23	0.35	0.11	0.23	0.07	0.04
SO3	0.01	0.01	<0.01	0.11	0.02	0.05	0.09	4.11
SiO2	40.22	47.56	41.59	54.2	74.49	63.43	73.57	73.7
SrO	0.03	0.02	0.11	0.1	0.02	0.03	0.02	0.03
TiO2	0.64	0.19	0.48	0.93	0.25	0.63	0.3	0.18

Table5.3. Trace elements analysis using inductively coupled plasma mass spectrometry method (assay values in ppm)

Elements	CAS-ICP-01	CCS-ICP-02	MG-ICP-03	A-ICP-04	MD-ICP-05	MGD-ICP-06	MGD-ICP-07	MGD-ICP-08	MGD-ICP-09	QV-ICP-10	MGD GC-01	MGD GC-06	MGD GC-08	MGD GC-11	MG GC-07	CAS GC-04	CCS GC-14	QV GC-05	QV GC-12	AP GC-13
Ba	145.50	770.00	96.20	264.00	87.20	31.70	163.50	147.00	220.00	109.00	467.00	252.00	370.00	520.00	68.80	32.00	31.90	1.20	5.40	445.00
Ce	10.20	4.20	3.50	12.10	5.00	9.80	5.20	13.00	6.80	9.50	13.60	11.90	9.90	45.40	14.30	11.00	13.20	0.50	<0.5	17.30
Cr	200.00	110.00	30.00	140.00	40.00	10.00	10.00	10.00	10.00	20.00	150.00	280.00	30.00	440.00	50.00	90.00	160.00	380.00	520.00	50.00
Cs	0.10	0.57	0.11	0.20	0.06	0.06	0.12	0.13	0.13	0.03	0.09	0.08	0.18	0.99	0.02	0.01	<0.01	<0.01	<0.01	0.17
Dy	1.57	1.48	1.43	1.82	2.44	5.33	2.03	3.08	0.78	5.26	4.31	2.46	4.24	3.96	6.52	10.15	2.14	<0.05	<0.05	7.03
Er	1.01	1.06	0.98	1.21	1.48	3.63	1.43	2.37	0.58	2.94	2.93	1.60	2.53	2.35	4.33	7.16	1.26	0.03	0.04	5.05
Eu	0.47	0.31	0.36	0.62	0.83	0.92	0.74	0.65	0.75	1.94	0.97	0.99	0.92	1.47	0.72	1.45	0.57	<0.03	<0.03	0.91
Ga	8.40	11.80	13.70	12.20	13.60	14.00	17.40	13.50	13.80	4.40	20.50	13.60	18.10	16.10	16.30	12.90	16.30	1.00	0.40	12.00
Gd	1.61	1.22	1.24	1.74	2.05	4.43	1.78	2.66	0.90	4.92	3.40	2.02	2.81	4.26	4.60	7.12	1.98	0.05	0.05	5.22
Hf	1.20	0.50	0.60	1.10	0.50	2.30	0.60	1.80	1.10	0.60	3.00	1.20	2.50	2.40	2.10	3.50	1.60	<0.2	<0.2	4.10
Ho	0.35	0.34	0.30	0.42	0.52	1.25	0.46	0.78	0.18	1.08	1.02	0.57	0.93	0.85	1.40	2.29	0.43	0.01	<0.01	1.55
La	4.80	1.60	1.30	5.40	2.00	3.70	2.10	5.70	3.30	2.90	5.50	5.30	3.90	20.80	5.20	3.50	6.00	<0.5	<0.05	7.00
Lu	0.12	0.17	0.15	0.18	0.26	0.53	0.19	0.40	0.09	0.32	0.51	0.30	0.33	0.36	0.76	1.08	0.18	0.01	<0.01	0.92
Nb	1.90	0.70	0.30	1.90	0.50	0.90	0.50	2.80	0.70	0.50	1.80	1.50	2.00	2.80	2.00	1.80	3.30	0.50	<0.2	2.30
Nd	6.40	3.30	2.70	6.40	4.10	8.00	4.10	7.10	3.50	8.00	9.40	7.00	7.10	24.70	11.70	10.80	7.60	0.10	0.20	13.10
Pr	1.40	0.65	0.54	1.55	0.77	1.55	0.83	1.65	0.85	1.61	1.79	1.52	1.35	5.42	2.06	1.77	1.65	0.03	<0.03	2.46
Rb	8.40	63.40	2.90	7.30	6.00	0.70	13.90	6.70	15.40	4.50	18.70	8.30	29.30	25.50	1.80	2.20	0.30	<0.02	<0.02	17.70
Sm	1.48	0.96	0.89	1.69	1.37	3.02	1.36	2.15	0.86	3.61	2.82	1.92	2.15	4.83	3.66	4.58	1.76	0.06	0.07	4.08
Sn	1.00	1.00	<1	<1	<1	1.00	<1	<1	<1	<1	1.00	1.00	<1	1.00	<1	1.00	<1	1.00	2.00	<1
Sr	100.50	319.00	455.00	222.00	198.00	111.00	425.00	160.50	205.00	147.00	378.00	354.00	306.00	312.00	284.00	159.00	443.00	8.30	1.70	172.50
Ta	<0.1	0.10	0.10	0.20	0.10	0.10	0.10	0.20	0.10	0.10	0.10	0.10	<0.1	0.10	<0.1	<0.1	<0.1	0.30	<0.1	0.10
Tb	0.25	0.22	0.22	0.27	0.34	0.82	0.31	0.46	0.14	0.88	0.62	0.39	0.61	0.66	0.89	1.41	0.33	0.01	0.01	1.00
Th	0.68	0.17	0.13	0.93	0.13	0.19	0.16	0.67	0.42	0.13	0.54	0.65	0.76	4.61	0.40	0.22	0.78	<0.05	<0.05	0.84
Tm	0.12	0.16	0.15	0.17	0.23	0.49	0.19	0.39	0.09	0.41	0.40	0.26	0.36	0.34	0.65	1.07	0.19	<0.01	<0.01	0.76
U	0.37	0.05	0.05	0.31	<0.05	0.09	0.06	0.30	0.13	0.09	0.21	0.17	0.22	0.93	0.15	0.12	0.40	<0.05	<0.05	0.25
V	128.00	209.00	358.00	156.00	145.00	37.00	422.00	8.00	32.00	22.00	60.00	13.00	99.00	244.00	308.00	31.00	264.00	24.00	<5	11.00
W	3.00	3.00	1.00	1.00	1.00	1.00	1.00	2.00	1.00	2.00	4.00	1.00	1.00	1.00	1.00	5.00	1.00	<1	1.00	2.00
Y	8.80	9.60	9.00	10.70	14.10	33.40	11.40	21.20	5.10	27.60	28.80	17.20	27.90	24.40	41.60	70.60	13.80	<0.5	<0.5	48.30
Yb	0.84	1.06	1.03	1.15	1.65	3.14	1.23	2.45	0.54	2.31	2.93	1.76	2.26	2.21	4.68	7.22	1.31	<0.03	<0.03	5.22
Zr	46.00	17.00	17.00	42.00	13.00	85.00	16.00	66.00	46.00	21.00	109.00	36.00	81.00	91.00	66.00	137.00	58.00	<2	<2	142.00

5.1. Analytical procedure

A lithium borate fusion of the sample prior to acid dissolution and ICP_MS analysis provides the most qualitative analysis approach for a broad suit of trace elements. The method adopted solubilizes most mineral species, including those that are highly refractory. Thirty elements package by lithium borate fusion and ICP_MS finish is analyzed by ALS global laboratory at Ireland. Re-bagging, sample weighing (WEI-21), pulp logging (LOG-24) is done in Addis Ababa head laboratory before shipment. An average weight of 100gm is taken from each sample. The purpose of preparation is to produce a homogeneous analytical sub-sample that is fully representative of the material submitted to the laboratory. A prepared sample (0.200 g) is added to lithium metaborate flux (0.90 g), mixed well and fused in a furnace at 1000°C. The resulting melt is then cooled and dissolved in 100 mL of 4% HNO3 / 2% HCl3 solution. This solution is then analyzed by inductively coupled plasma - mass spectrometry. The lithium metaborate fusion is not the preferred method for the determination of base metals. Many sulfides and some metal oxides are only partially decomposed by the borate fusion and some elements such as cadmium and zinc can be volatilized. Some base metal oxides and sulfides may not be completely decomposed by the lithium borate fusion. Results for Ag, Co, Cu, Mo, Ni, Pb, and Zn will not likely be quantitative by ICP_MS method.

No single analytical method is able to encompass the full range of elements required for effective lithogeochemical investigation, X-ray fluorescence can be used for major rock-forming elements following a fusion. Whole rock analysis related to lithogeochemistry, minerals alteration, and trace element mobility are important tools for understanding ore-forming geological environments. A prepared sample (0.66 g) is fused with a 12:22 lithium tetraborate –lithium metaborate flux which also includes an oxidizing agent (Lithium Nitrate), and then poured into a platinum mold. The resultant disk is in turn analyzed by XRF spectrometry. The XRF analysis is determined in conjunction with a loss-on-ignition at 1000^0C. The resulting data from both determinations are combined to produce a "total". Aluminum, Barium, Calcium, Chromium, Iron, Potassium, Magnesium, Manganese, Sodium, Phosphorous, Sulphur, Silicon and Titanium oxides abundance are determined by this method.

Managing and interpreting large datasets generated by lithogeochemical techniques, while traditionally challenging, have been greatly simplified by powerful software tools now available to geologists and geochemists. Geochemical interpretations are conducted using the conventional binary and ternary discrimination diagrams. Geochemical data interpretations for the formerly mentioned discriminations are processed using plot diagrams generated by Petrograph ver.1.0.5 software and Microsoft Excel application.

5.2. Source rock determination

The Y/Nb ratios of all core samples taken from the study area are greater than one (4.6, 13.7, 30, 5.6, 28.2, 37.1, 22.8, 7.57, 7.28, 55.2, 16, 11.4, 13.95, 8.71, 20.8, 39.2, 4.18, 1, 2.5, 21), which is considered to be a characteristic of magmas with transitional to sub alkali composition (Pearce & Cann, 1973).

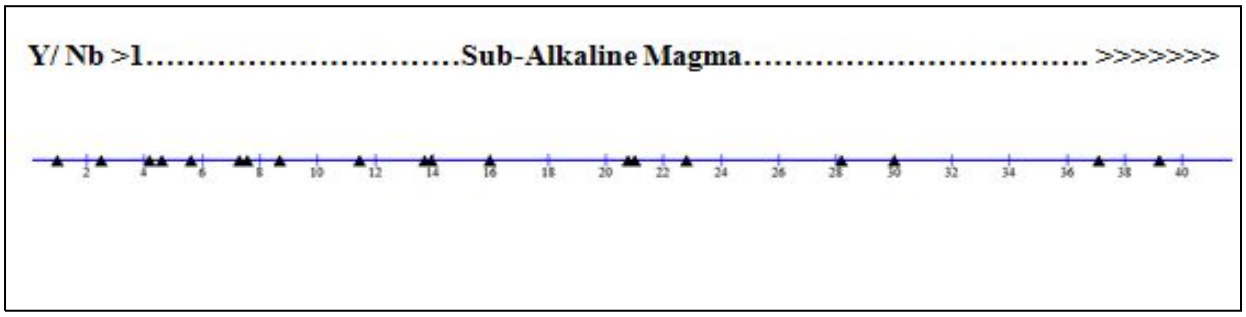

Figure5.1. Y/Nb ratio diagram for discrimination of magma; after Pearce & Cann (1973)

Triangular variation diagrams are used when it is necessary to show simultaneous change between variables. The AFM diagram is the most popular triangular variation diagrams and takes its name from the oxides plotted at its apices; alkalis (Na_2O+K_2O), Fe oxides ($FeO+Fe_2O_3$) and MgO. The AFM diagram is most commonly used to distinguish between tholeiitic and calc-alkaline differentiation trends in the sub-alkaline magma series. Kuno (1968) and Irvine and Baragar (1971) present dividing lines separating the rocks of the calc-alkaline series and rocks of tholeiitic series. Kuno's line boundary yields a smaller area for the tholeiitic suite.

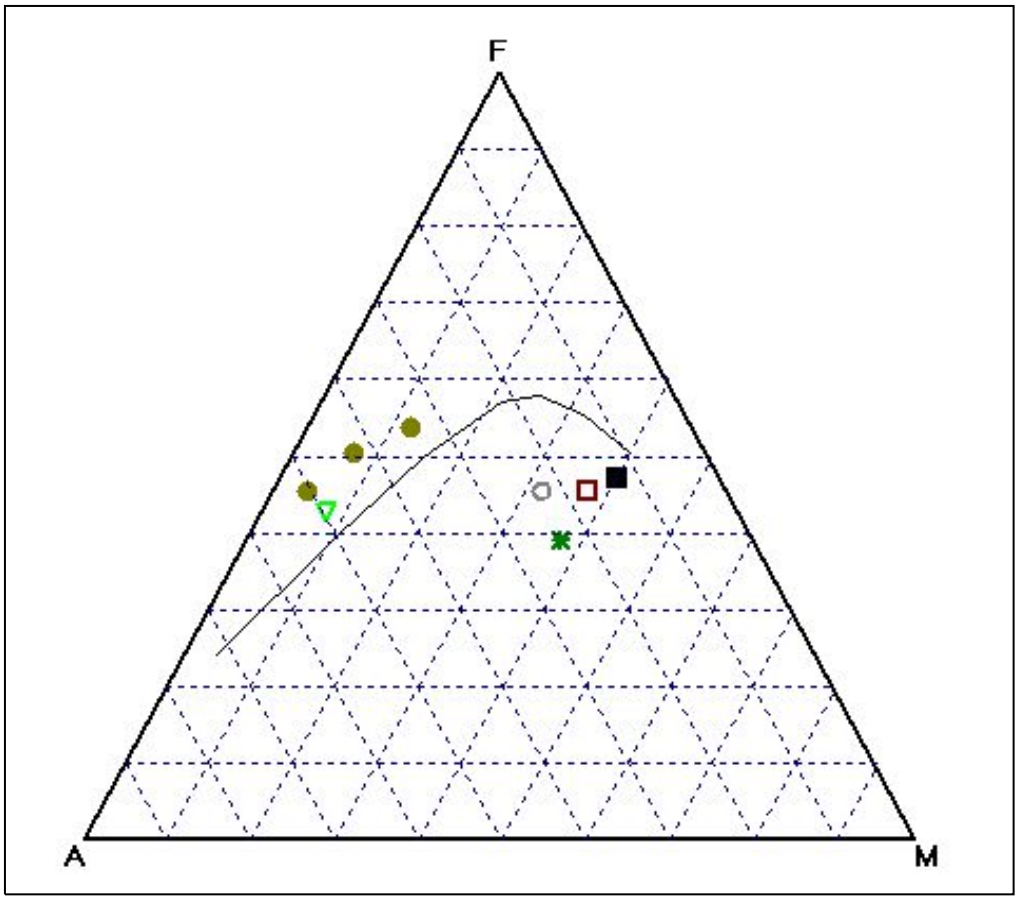

LEGEND	CAS	CCS	MG	A	MD	MGD

Figure5.2. A-F-M diagram for discrimination of sub-alkaline magma; after Kuno(1968)

The division of tholeiitic and calc-alkaline series of magmas is further identified using AFM ternary discrimination diagram. Metagranodiorite and metadiorite rock units lie in the tholeiitic region of the AFM ternary diagram. The granitoids are found tholeiitic in composition while the prothloith originated from calc-alkaline source magma series. The plot diagram clearly verified that, the source rock of granodiorite is tholeiitic ocean crust.

The total alkalis-silica diagram is one of the most useful classification schemes available for volcanic rocks. The usefulness of the TAS diagram was demonstrated by Cox et al, (1979), who showed that there are sound theoretical reasons for choosing SiO_2 and $Na_2O + K_2O$, as a basis for the classification of volcanic rocks. The TAS diagram divides rocks into ultrabasic, basic, intermediate and acidic on the basis of silica content. The TAS classification scheme is intended

for the more common, fresh volcanic rocks. It is inappropriate for potash-rich rocks and highly magnesian rocks and should not be normally used with weathered, altered or metamorphosed volcanic rocks because the alkalis are likely to be mobilized. Rocks showing obvious signs of crystal fractionation should also be avoided. TAS for plutonic rocks Wilson (1989) uses the diagram for classification of plutonic igneous rocks. This diagram is of great practical use for there is no other classification of plutonic rocks.

Discrimination between the alkaline and sub-alkaline rock series using TAS volcanic rocks may be subdivided into two major magma series; the alkaline and sub-alkaline series.

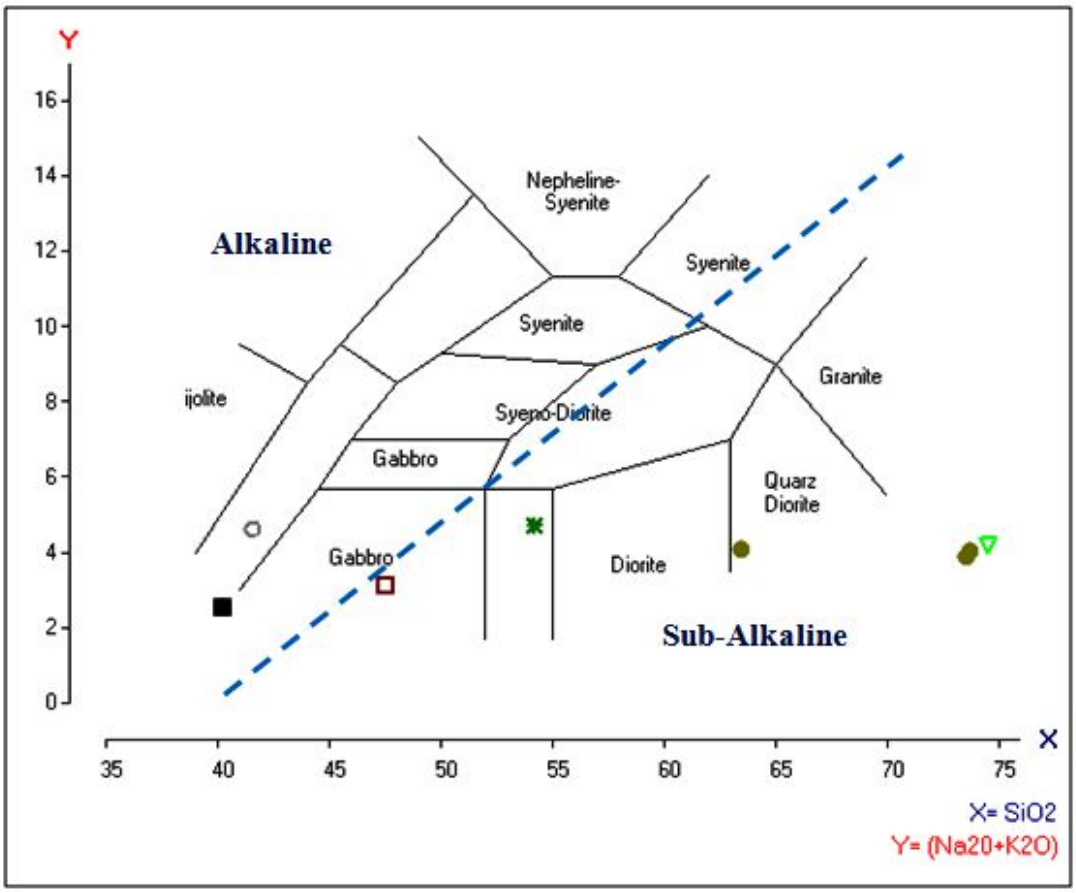

LEGEND	■ CAS	□ CCS	○ MG	✳ A	▽ MD	● MGD

Figure5.3. The chemical classification and nomenclature of plutonic rocks using the TAS (Na2O+K2O Vs SiO2) diagram; after Cox-Bell-Pank (1979) adopted by Wilson (1989). The dotted line subdivides the alkali from sub-alkali rocks.

Total alkali versus silica discrimination diagram is adopted to verify the rock signature and further outline the specific identification of the major rock units of the area. The plot diagram re-assures that most of the province lithologies are sub-alkaline magma in origin. The acidic intrussives lie in the range of quartz-diorite (granodiorite) to granite in composition while most of the mafic metavolcanics are found to be gabbro-amphibolite in composition (Figure 5.3).

The classification system outline by Chappel & White (1974) was proposed initially to divide granites into *I-type* (or igneous protolith) and *S-type* (or sedimentary protolith) granite. Both of these types of granite are formed by melting of high grade metamorphic rocks, either other granite or intrusive mafic rocks, or buried sediment, respectively. I- and S-type subdivision is not simply one that refers to source rocks of different compositions, but also to source rocks of fundamentally different origins, involving prior infracrustal and supracrustal origins. The infracrustal I-type granite originated at a deeper crustal level while the supracrustal S-type granite originated at shallower crustal depth. Petrographically, I-type granite posses hornblende and muscovite mica. The S-type granite is distinct with the appearance of K-feldspar and biotite mica. According Sha-Chappel (1999) classification criteria, for I-type felsic rocks La/Y ratio lies between 0.05-0.29 and Sm/Nd ratio lies between 0.29-0.58. Seven out of nine acidic intrusive rocks lied in the given interval of (La/Y) ratio (0.14, 0.11, 0.18, 0.26, 0.19, 0.3, and 0.13) while six out of nine of (Sm/Nd) ratio lied in the interval (0.334, 0.37, 0.331, 0.3, 0.3, and 0.3). From the results we can suggest the felsic metavolcanics are I-type granite.

S-type granites always contain more Al than the amounts of Na, Ca and K in the rock required forming feldspars, primarily owing to their derivation from source components that had previously been weathered. Those rocks are therefore always saturated in Al, or peraluminous. Many I-type granites are also peraluminous, despite I-type source rocks typically not being saturated in Al. It has previously been suggested that this may result from the fractional crystallisation of amphibole. However, data from compositionally zoned high-temperature plutons show that it is difficult to generate large quantities of peraluminous melt by removal of amphibole. Most of the I-type granites formed at lower temperatures and almost half of those rocks for which bulk chemical compositions are available are peraluminous. Fractional crystallisation of mafic magma is inefficient for forming peraluminous granites. Peraluminous

granites can form by partial melting of metaluminous crustal sources (Bruce W. Chappell etal; 2012).

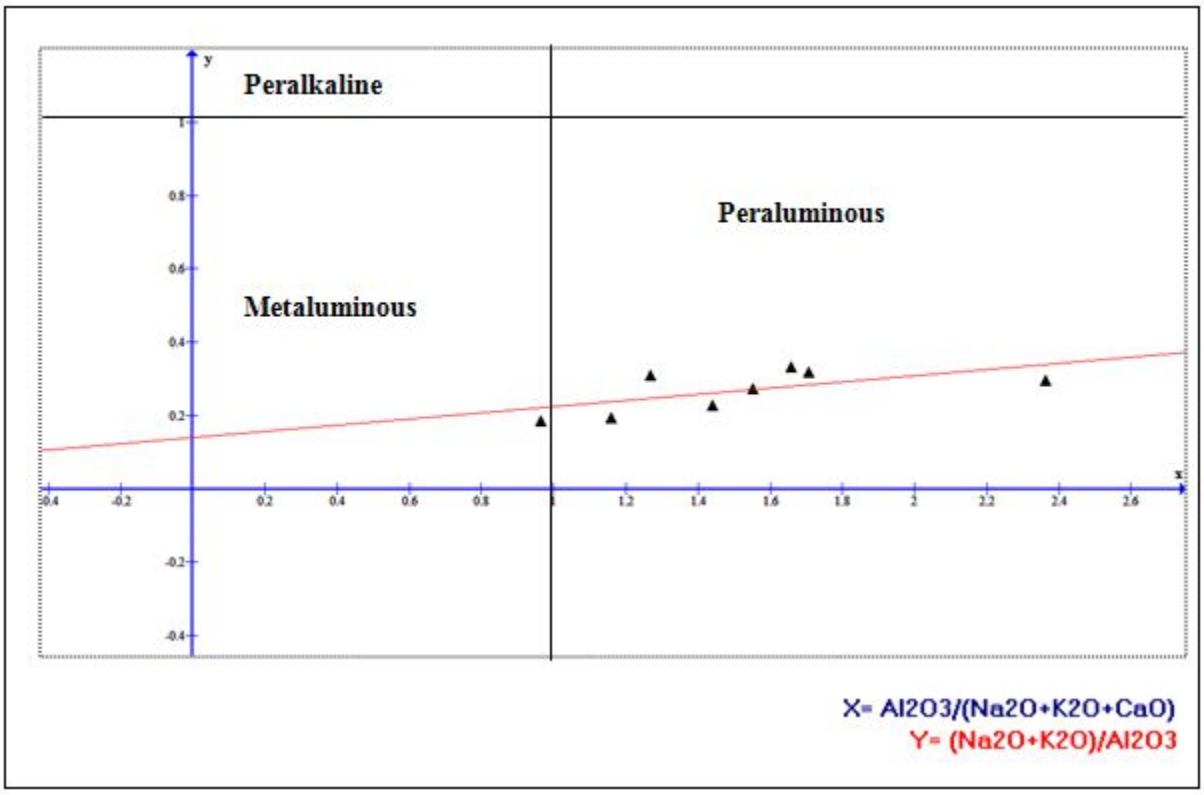

Figure5.4. NK/A vs. A/NKC diagram of Shand (1943) discriminating metaluminous, peraluminous and peralkaline compositions

Peraluminous rocks are igneous rocks that have a molecular proportion of aluminium oxide higher than the combination of sodium oxide, potassium oxide and calcium oxide. Alumina saturation indices showed that Okote metavolcanics lie in the region where $Al_2O_3/(Na_2O+CaO)>1$ and $(Na_2O+K_2O)/Al_2O_3<1$. Approximately all of metavolcanics of the Okote prospect are peraluminous.

The granitoids are enriched of Na_2O due to the existence of Albite plagioclase in the felsic intrusive. Lower K_2O in the granodiorite suggests depletion of orthoclase which is petrographic characteristics of I-type granite. Fe_2O_3 and MgO are less abundant in the metagranodiorite while the mafic metavolcanics are enriched with these oxides. The enrichment of CaO in the mafic rocks explains the presence of Anorthite plagioclase. All metavolcanics have similar abundance

of Al_2O_3 and yet proofed to be peraluminous in composition. The occurrences of Al_2O_3 in all feldspars (albite, anorthite and orthoclase) highly contribute for the entrance to alumina rich composition.

5.3. Tectonic setting

The number of tectonic environments recognized today is much greater than 20 years ago. This reflects the advances made in understanding both earth processes and the chemistry of igneous rocks. Pearce and Cann (1971, 1973) originally identified the geochemical signature of rocks from volcanic-arcs, from the ocean floor and from within plates.

Discrimination diagrams seldom provide an equivocal confirmation of a former tectonic environment. At best they can be used to suggest an affiliation. They should never be used as a proof. Furthermore, discrimination diagrams were never be used for single samples, but rather with a suite of samples to eliminate the occasional spurious result and highlight data-sets from mixed or multiple environments. By taking into consideration of the precaution, twenty samples have been applied for the discrimination of the tectonic environment of the area of interest.

There are a large number of discrimination diagrams applicable to basalts and basaltic andesites which use trace elements, major and minor elements and the mineral clinopyroxene. From the list of elements in the analysis table (Table 5.3), the elements Rb, Y (and its analogue Yb) and Nb (and its analogue Ta) were selected as the most efficient discriminants between types of oceanic-ridge granite, within-plate granite, volcanic-arc granite and syn-collisional granites. Post-orogenic granites cannot be distinguished from volcanic-arc and syn-collisional granites on the diagrams below. Supra-subduction zone granites can only be identified successfully when there is geological evidence from an ocean setting. They may be then identified on an Nb-Y diagram from their lower Y content, which is not actually in our case.

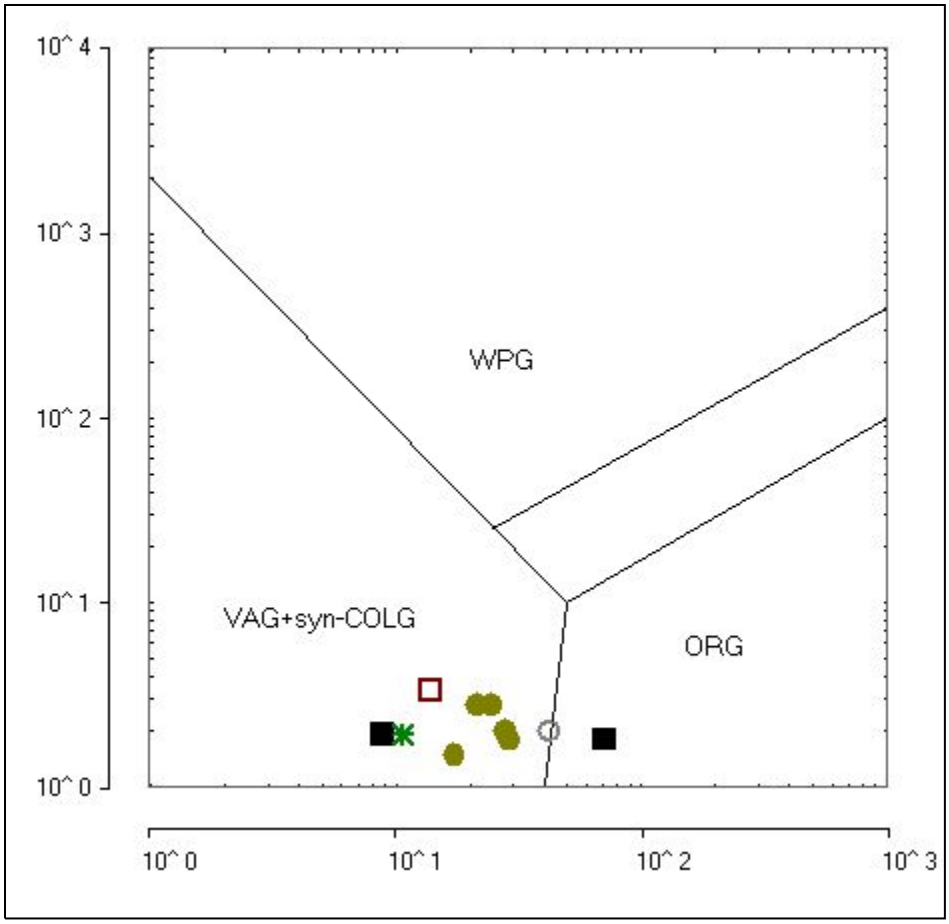

Figure5.5. Graph showing tectonic discrimination using Log (Nb) vs. Log (Y); after Pearce (1984); X-axis =Y & Y-axis=Nb

A bivariate plot of Nb and Y can be subdivided into three fields into which Oceanic granites (ORG), within-plate granites (WPG) and volcanic-arc granites (VAG) together with syn-collisional granites (syn-COLG) plot (Figure 5.5).

Nb-Y binary discrimination diagram showed that all of the analyzed samples lie in VAG+syn-COLG (i.e. Volcanic arc granites + syn-collision granites) region. Therefore we can suggest that the tectonic environment is subduction zone which is in good agreement with Woldehaimanot and Behrmann (1995) regional analysis of Adola belt.

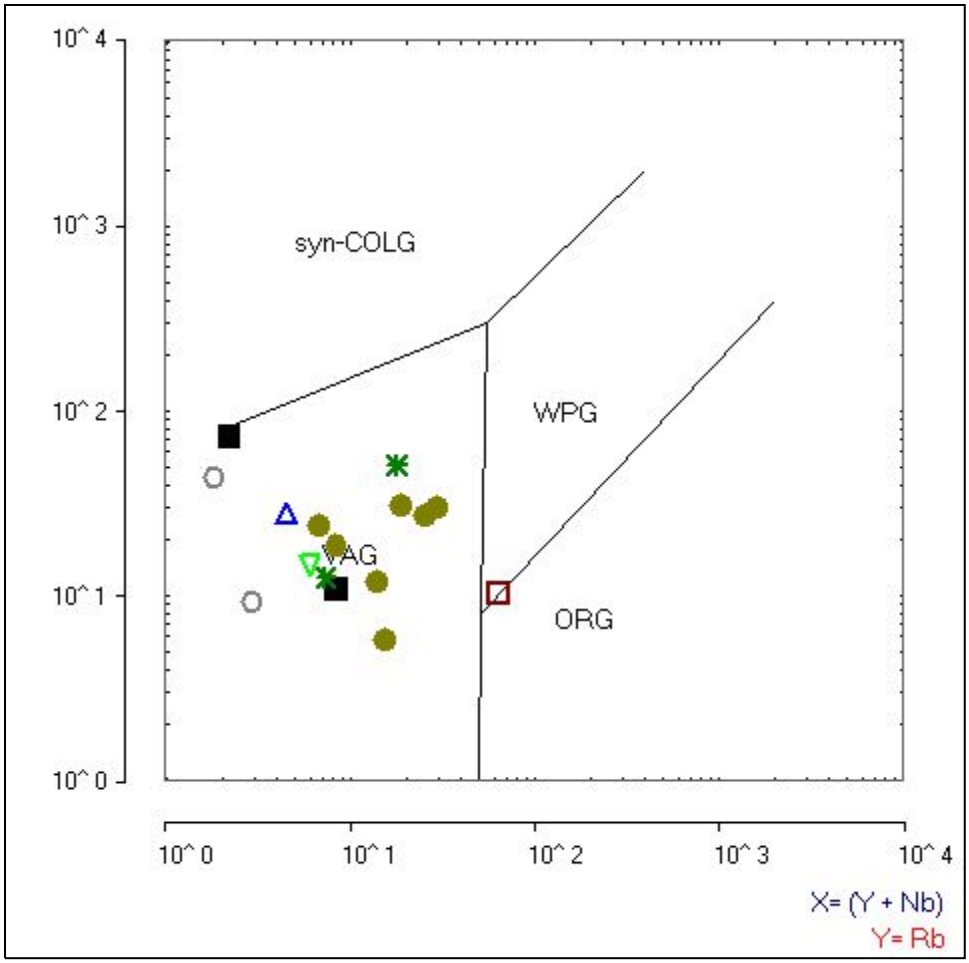

LEGEND	■ CAS	□ CCS	○ MG	✳ A	▽ MD	● MGD	△ QV

Figure5.6. Graph showing tectonic discrimination using Log (Y+Nb) vs Log (Rb); after Pearce (1984)

A bivariate plot Rb and (Y+Nb) more efficiently separates syn-collisional granites from volcanic-arc granites. There is also a clear division between within-plate and oceanic granites on this diagram (Figure 5.6).

Log-Log Y+Nb Vs Rb plot diagram for granites distinguish VAG from syn-COLLG. The binary plot diagram demonstrated the metavolcanics of the prospect are identified to be volcanic arc granite (VAG). The volcanic arc granite tectonic setting is a suitable site for the origin of I-type granite.

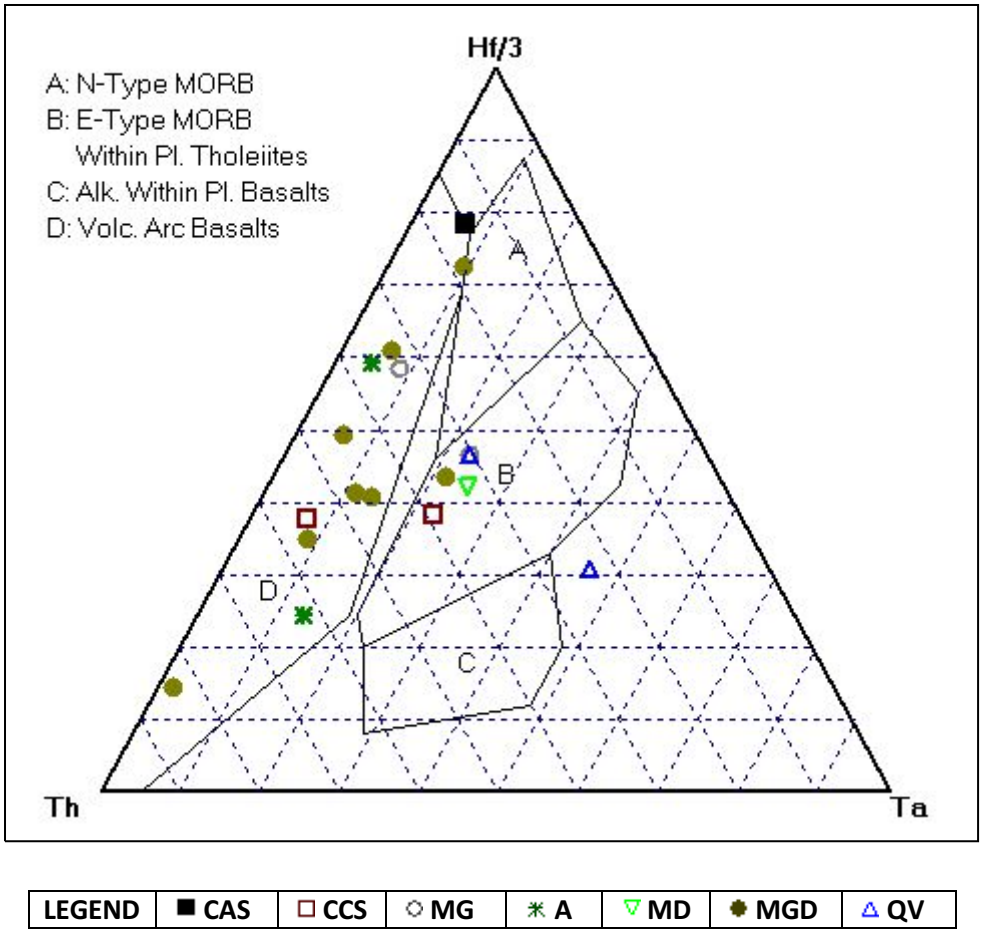

Figure5.7. Graph showing tectonic discrimination using Th –Hf/3- Ta; Wood (1980)

A discrimination diagram based upon the immobile HFS elements Th-Hf-Ta was proposed by Wood (1980). In order to expand and center the fields of basalt types, concentration are plotted (in ppm) as Th, Hf/3 and Ta. The elements Th, Hf and Ta are present in very low concentrations in basalt and cannot be accurately determined by XRF analysis so must be determined by ICP-MS. The Th-Hf-Ta ternary plot diagram is applied to address the tectonic setting of mafic metavolcanics and yet demonstrated to be volcanic arc basalt (VAB).

5.4 Spider diagrams

5.4.1. REE pattern

The rare earth elements are regarded as amongst the least soluble trace elements and are relatively immobile during low grade metamorphism , weathering and hydrothermal alteration (Michard 1989). Therefore, hydrothermal activity is not expected to have a major effect on rock chemistry unless the water/rock ratio is very high. However, the REE pattern are not totally immobile, therefore attention should be given in interpreting heavily altered or highly metamorphosed rocks. Nevertheless REE patterns, even in slightly altered rocks, can faithfully represent the original composition of the unaltered parent and a fair degree of confidence can be placed in the significance of peaks and troughs and the slope of a REE pattern (Hugh. R. Rollinson , 1993).

The rare earth elements pattern of an igneous rock is controlled by the REE chemistry of its source and the crystal melt equilibria which have taken place during its evolution. Trace elements analysis is done on representative twenty core samples from metagranodiorite, metadiorite, metagbbro, amphibolite, chlorite-amphibole schist and quartz vein representing the metavolcanics of the area.

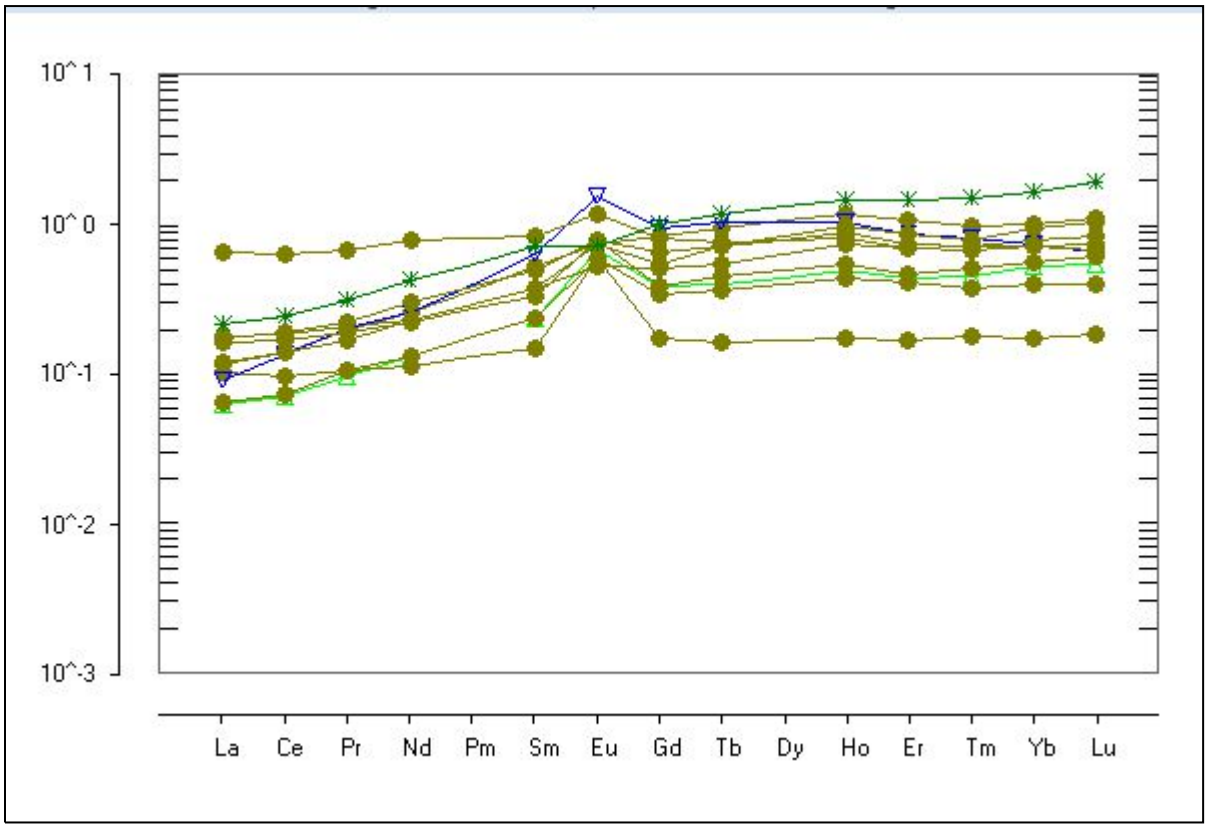

LEGEND	▽ MD	● MGD	△ QV

Figure5.8. Chondrite-normalized REE pattern for felsic metavolcanics, normalization values are from NASC- Haskin & Haskin (1966)

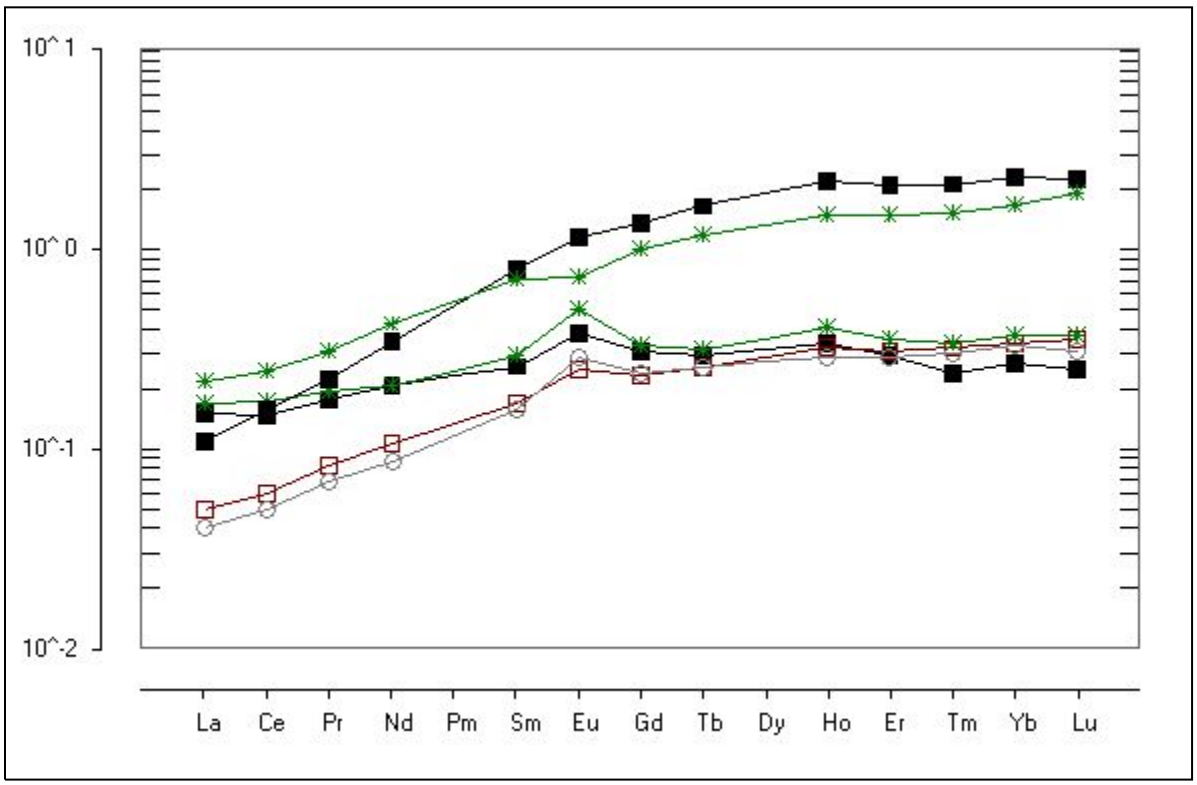

LEGEND	■ CAS	□ CCS	○ MG	✳ A

Figure5.9. Chondrite-normalized REE pattern for mafic metavolcanics, normalization values are from NASC- Haskin & Haskin (1966)

The chondrite-normalized spider diagrams above showed the rare earth elements pattern of felsic and mafic metavolcanics of the prospect area (see Figure 5.8 & 5.9). A positive Eu anomaly is observed on the felsic metavolcanics REE pattern. The positive Eu anomaly in the felsic REE pattern suggests the enrichment of calcic-plagioclase interpreted as crustal contamination during interaction of magma with the upper mantle at the conveyor belt. The slight positive Eu anomaly of the mafic metavolcanics is a usual phenomena which occurred as a result of anorthite. REE pattern of mafic rocks shows considerable enrichment of HREE and depletion of LREE by forming a gentle slope i.e. $(La/Yb)_N<1$ while felsic intrusives exhibit flat pattern. The granitoids do not show fractionation while mafic protholith moderately fractionated. Zircon will have an

effect similar to that of garnet and will deplete HREE; hence the slight enrichment of HREE in the mafic rocks indicates the depletion of zircon. The slight depletion in the LREE might suggest the occurrence of monazite or allanite in the protholith.

5.4.2. Multi-element diagram for igneous rocks

MORB-normalized spider diagrams are most appropriate for evolved basalts, andesites and crustal rocks, rocks to which MORB rather than primitive mantle could be parental. This form of spider diagram was proposed by Pearce (1983) and is based on two parameters. Firstly, ionic potential is used as a measure of the mobility of an element in aqueous fluids. In terms of this, LILE are highly mobile. Secondly, the bulk distribution coefficient for the element between garnet lherzolite and melt is used as a measure of the incompatibility of an element in small degree partial melts. The elements are ordered so that the most mobile elements (Sr, K, Rb, Ba) are placed at the left of the diagram and in the order of increasing incompatibility. The LILE group is followed by HFSE group (Th, U, Nb, Ta, Nd, Zr, Hf, Tb, Y). Although Ce is LILE group, due to its immobility it is normally plotted in the HFSE group.

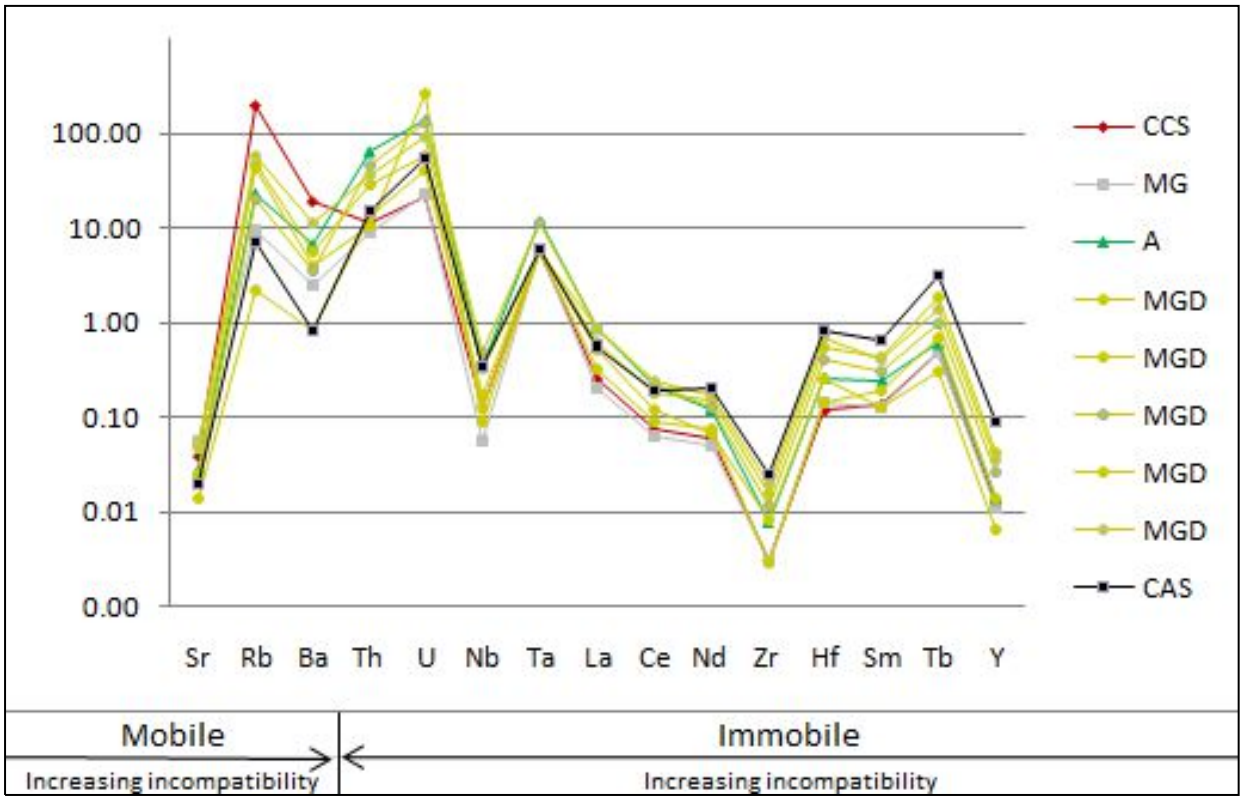

Figure5.10. MORB normalized multi element diagram pattern of Okote metavolcanics, normalization values are from Pearce, J.A. and Parkinson, I.J., (1993)

Multi-element diagrams contain a more heterogeneous mix of trace elements than do REE diagrams. Consequently they often show a greater number of peaks and troughs reflecting the different behavior of different group of trace elements. The contrasting behavior of the more mobile LILE with the less mobile HFSE can be a good explanation for the roughness of the diagram. On the one hand LIL elements concentration are a function of the behavior of a fluid phase, whilst HFS element concentrations are controlled by the chemistry of the source and the crystal/melt processes which have taken place during the evolution of the rock (Hugh. R. Rollinson, 1993).

Abundance of elements are strongly controlled by individual minerals. Zr depletion is due to the absence of zircon mineral which was also shown by HREE enrichment of the protholith. Negative Nb anomalies are also characteristics of the continental crust and may be an indicator of crustal involvement in magma process.

The existence of sphene is evidenced by the positive Ta anomaly. More mobile LILE element concentrations (Ba & Rb) may be controlled by aqueous fluids but these elements are concentrated in the continental crust and can also be used as indicator of crustal contamination of magmas. Ba and Rb enrichment in carbonate chlorite schist confirms the existence of metasomatism responsible for the shear hosted gold mineralization.

CHAPTER SIX

6. FLUID INCLUSION

Ore minerals, like any other minerals and rocks crystallize from fluids (liquid and vapor). However, the fluids are not present at the time of ore deposit study. We therefore depend on indirect sources of information to study the nature, source, physical and chemical condition of deposition and other information about the original fluids, ore components and depositional environments. Such information is extracted from materials contained inside the ore minerals and their associates. Among these important sources of information fluid inclusions are the main ones.

Fluid inclusions are fluids trapped in tiny cavities during growth of crystals. They contain one or more phases (solid, liquid, or vapor) trapped as impurities within minerals. Their sizes range from sub-microscopic up to several hundred micrometers in diameter, and their masses are typically in the order of nano grams. Where they are enclosed by transparent minerals (like quartz, fluorite, halite, calcite, apatite, dolomite, sphalerite, barite, topaz and cassiterite), fluid inclusions may be observed in a microscope using polished sections or doubly polished thin sections of the host minerals. Various sources of evidence suggest that many fluid inclusions preserve the chemical and physical properties of the original parent fluids from which they formed. This is based on the assumptions that no other deposition of external fluids and no leakage/loss of the original fluid inclusion were present. Fluid inclusions are therefore considered to be direct samples of the ore-bearing fluids, and their chemical analysis provides information on the: source and character of ore fluids, source of the ore constituents ,fluid migration, ore transport and deposition, complexing ligands for metal transport and concentration, and temperature of deposition. Studies on fluid inclusions in the past revealed that the dissolved salts (as much as 70% of the liquid by weight) are primarily chlorides, sulfates, and carbonates of Na, K, Mg and Ca. Among these Na and Cl are the most abundant dissolved salts. This indicates that halides play the biggest role in ore genesis and fluids were highly saline hot aqueous solutions (Roedder & Bodnar, 1997).

Fluid inclusions have been used as a crucial source of geothermometric data. This is done by heating the mineral until a single phase of the fluid inclusion is restored. This homogenization temperature is taken as the minimum temperature of entrapment of the original fluid. The actual temperature of deposition can be estimated after correcting this value for pressure (depending on fluid density and salinity). Moreover, fluid inclusions show the physical state of fluids during deposition (whether boiling took place or not). This is known if gas-rich and gas-poor aqueous inclusions are found together. In order to deduce the composition of the ore-bearing fluids, the inclusions must be chemically analyzed. Fluid inclusions are divided into primary, secondary and pseudo-secondary and the study should start by identifying which one of these is present in the sample so that reliable information on the original fluid is collected. The commonest fluid inclusions in ore deposits are grouped into four compositional groups; these are moderately saline, gas rich inclusion, halite bearing inclusions and CO_2-rich inclusions (Bodnar, 2003).

Understanding the fluid inclusion behavior of quartz mineral hosted by granodiorite rock unit of Okote area clarifies the type of fluid responsible for the genesis of intrusive related disseminated gold mineralization.

6.1. Fluid inclusion petrography

Four samples (J36, J44, J47 and J57) are collected from quartz veins related to granodiorite disseminated gold mineralization for fluid inclusion petrographical study using transmitted light microscopy. Petrography is done at Burlinson laboratory to enrich the understanding and identification of fluid inclusion. The two samples are from Okote while the others are from Wayu Boda and Horoto prospects.

Table6.1. Description of wafer sections for FI petrographical study

#	Analysis	Lithological Description	Sample Code	J Series	Prospect area	Sample Type
1	Fluid Inclusion	Banded granodiorite with semi translucent pale grey quartzose zones & grey mafic	FI-OK-13	J36	Okote	Core
2	Fluid Inclusion	Coarse, semi translucent white qtz, much CR removed during preparation	FI-OK-15	J44	Okote	Core
3	Fluid Inclusion	Light brown granite and much green mineral (malachite) with coarse transparent qt	FI-HO-04	J47	Wayu Boda	Chp
4	Fluid Inclusion	Banded fine grained light brown qtz and med grained white felspar, 80% qtz, no mafic	FI-WB-05	J57	Horoto	Chip

Fluid inclusion petrographic examination of the above four samples was performed at Burlinson geochemical laboratory. The observation was done on crushed grains in refractive index oil. There were very few FIs which could be certain were primary, and almost all inclusions are less than 5 microns and hard to see in crushed grains.

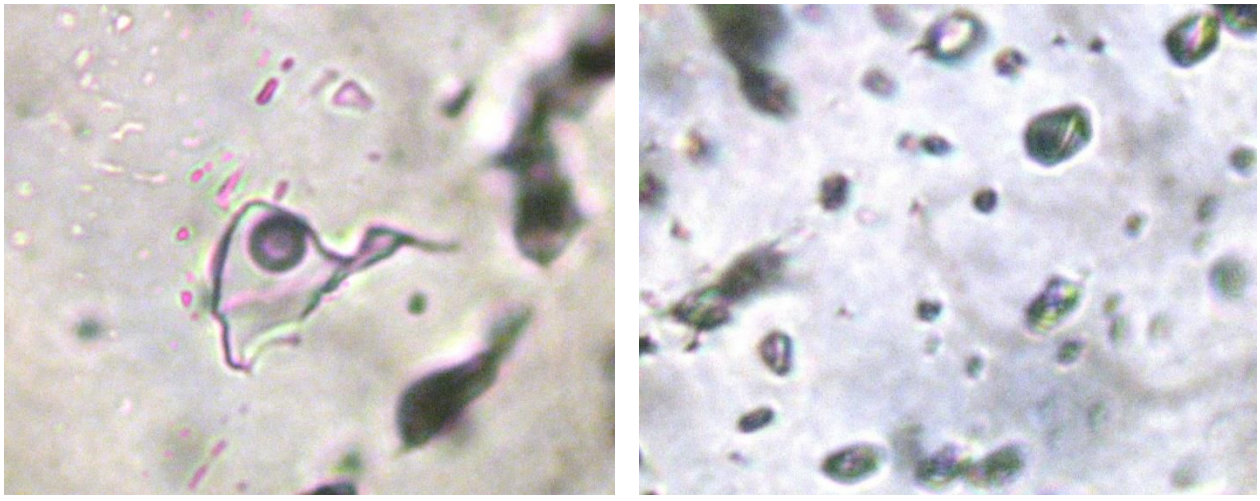

A (J44) **B (J36)**

Plate6.1. Auriferous quartz vein and granodiorite hosted fluid inclusion: a) spheroidal type I two phase aqueous inclusions; b) negative crystal shape type I

Type-I fluid inclusion is moderately saline inclusion containing two phases. The dominant phase is water followed by bubbles of water vapor constituting 10-15% of the inclusion. The presence of bubbles is indicative of trapping at an elevated temperature with the formation of the bubbles on cooling.FI is not Type-II which is gas rich inclusion (generally >60% vapor). Unlike the shear hosted gold mineralization there is no segregation of CO_2 from the vapor phase, which is another

evidence for the absence of acidic hydrothermal fluid. FI is not Type-IV which are CO_2-rich inclusions. Type-III is halite bearing inclusions. They have high salinity ranging up to more than 50%. Sample (J44) for petrographic study clearly outlined that FI is Type-I which is characterized by moderately saline inclusion containing two phases (dominant liquid and vapor), which suggests magmatic hydrothermal fluid which is evidenced by 10-15% vapor constitute and lack of CO_2 segregation.

6.2. Baro-acoustic decrepitation

The decrepitation method was used in the early days of fluid inclusion research. The method heats a sample of crushed mineral grains and "listens" to "explosions" as the pressure builds up within the inclusions and bursts the inclusions open. The result is a histogram of decrepitation counts versus temperature. Baro-acoustic decrepitation is a simplified method to obtain reproducible, non-subjective fluid inclusion data quickly and without the need for polished thin sections or microscopes. It can provide information about the source fluid environment and targeting vectors on project-scale numbers of samples, at modest price and with quick analytical turnaround. The most important use of the analytical method is in determining approximate total gas contents of samples, as this data is frequently closely correlated with mineralisation potential. Examples in this documentation show this use as well as others including the discrimination between samples which are visually identical and in discerning temperature zonation effects within a vein, mine or small exploration area. It can even be used on opaque minerals where microscopy is completely impossible, and many examples from iron oxide minerals are shown here. This method was wrongly discredited by early work in the 1950's in Canada at a time when the presence of gas-rich fluids in hydrothermal systems was not understood and neither was the thermodynamic behavior of such fluids within inclusions. With the benefit of our currently much improved understanding of fluid systems it is now clear that baro-acoustic decrepitation does in fact provide a very useful and practical mineral exploration technique, particularly given the ability to digitally automate the instrumentation as has been done. The method is not intended to compete with the very high accuracy of slow and painstaking microscopic fluid inclusion research. Decrepitation instruments are currently in use in China and a modern computer controlled digital instrument is used by Burlinson Geochemical

Services, described here. However, as with soil geochemical surveys, where low cost and speed are more important than extreme accuracy, baro-acoustic decrepitation has a valuable role to play in many types of exploration program. Although the method is usually applied to quartz samples, it has been used on various minerals including sulphides, haematite, magnetite, fluorite, carbonates and jasperoids. Conventional academic methods of analyzing fluid inclusions are too slow and tedious to be of practical application in typical mineral exploration activities. A particularly useful fluid parameter to know is the CO_2 content, because there are numerous case studies in the literature which clearly document a strong correlation between CO_2 content and gold mineralisation at many deposits. The baro-acoustic decrepitation method is the easiest way to obtain CO_2 information. It can be used on large numbers of samples to quickly provide a spatial array of data which is necessary for exploration applications. If fluid inclusions contain a significant gas content, CO_2 or CH_4, then the decrepitation histogram has a characteristic low temperature peak below 300 to 350 C. This is because these gases do not condense to a liquid phase, as water does, and will rapidly generate high pressures when the sample is heated, leading to premature decrepitation. This effect is well known from microthermometric studies which often note the premature decrepitation of inclusions before homogenization. Decrepitation can also be used to estimate the fluid temperatures from which samples formed, although the results are more difficult to interpret and are best used only to define relative temperature variations across a spatial suite of samples. The temperatures are however highly reproducible and representative of the entire sample and of numerous fluid inclusions, overcoming some serious limitations of the microthermometric determination of fluid temperatures. The method is the most practical method to determine temperatures of the large numbers of samples required. Salinities of fluid inclusions are of limited use in exploration and are difficult to measure. However, they can be used to recognize intrusion related hydrothermal systems. This method works best with dense fluids. Epithermal fluids, formed at near surface conditions are usually of low density and give weak decrepitation responses. The analytical method does not provide salinity information (Burlinson, K. 2012)

Fifteen samples are collected from quartz veins in relation to intrusive related disseminated gold mineralization for understanding the temperature of formation so that to suggest the existence of

porphyry or other type mineralization and shipped to the laboratory for analysis. The analysis is done at Burlinson geochemical services located at Australia.

Small whole rock quartz samples of 10 gm weight each are collected and shipped by DHL to its final destination. The sample is reduced to 0.5 gm of crushed rock grains sieved to -420+200 micron from monometallic quartz mineral to avoid misleading from other minerals. The samples proceed to analysis to determine the decrepitation by subjecting to temperature gradually increasing from 100 to 620^0C at a rate of 20 degree per minute which enables to understand the approximate temperature of origin.

Table6.2. Field samples description for baro-acoustic decrepitation method

#	Drill hole	X	Y	Depth (m)	Sample code	Remark
1	DH1125N/2	474742.0	565670.5	134	FI-OK-01	MGD
2	DH1700N/3	475081.5	566209.3	110.5	FI-OK-02	QV
3	Wayu Boda	468395.0	551025.0	Surface	FI-WB-03	MGD
4	Horoto	500609.0	523458.0	Surface	FI-HO-04	Granite
5	Wayu Boda	468350.0	550882.0	Surface	FI-WB-05	MGD
6	Horoto	500425.0	523439.0	Surface	FI-HO-06	Granite
7	DH800N/1	474485.3	565410.1	95	FI-OK-07	MGD
8	DH800N/1	474485.3	565410.1	122	FI-OK-08	QV
9	DH900N/1	474503.5	565511.1	210	FI-OK-09	MGD
10	DH900N/1	474503.5	565511.1	260	FI-OK-10	MGD
11	DH900N/1	474503.5	565511.1	263	FI-OK-11	QV
12	DH1300N/1	474822.6	565872.7	88.5	FI-OK-12	QV
13	DH1200N/1	474776.2	565727.6	182	FI-OK-13	MGD
14	DH1650N/2	474979.2	566190.3	67	FI-OK-14	QV
15	DH1700N/3	475081.5	566209.3	45	FI-OK-15	QV

The J series refers to recently improved decrepitometer model 215 which is about five times more sensitive than the older H-series data (models 105 and 205) is applied for this study. This does not affect temperature measurements, only intensity measurements. Description of hand sample and coding of laboratory sample numbers are done at Burlinson laboratory by listing from 2046 to 2059.

Table6.3. Cross referenced sample description and laboratory observation

J series	LAB. CODE	FIELD CODE	Sample description	REMARK
J24	2046	FI-OK-01	Pale greenish Qtz-Felspar + 20% nmafics	
J25	2047	FI-OK-02	Semi-translucent white qtz, minor S=	
J26	2048	FI-OK-07	Pale greenish-gray granodiorite with much S=, very fine grain minor mafics,	
J27	2049	FI-OK-08	Opaque milky white quartz	
J28	2050	FI-OK-09	Fine grained, pale grey, speckled granodiorite, 10% mafics	suspiciously intense – noise coupling ; repeated J59
J29	2051	FI-OK-10	Medium grained spotted pale grey granodiorite, S= on fracture planes, maybe 2%	
J30	2052	FI-OK-11	Semi translucent white qtz with muscovite. dark grey country rock removed in preparation	
J36	2054	FI-OK-13	Banded granodiorite with semi translucent pale grey quartzose zones & grey mafic	
J43	2055	FI-OK-14	Coarse, slightly translucent milky white qtz	
J44	2056	FI-OK-15	Coarse, semi translucent white qtz, much CR removed during preparation	
J47	2057	FI-HO-04	Light brown granite and much green mineral (malachite) with coarse transparent qt	
J49	2058	FI-HO-06	Very coarse, qtz dominant granite, trace green (malachite), pink feldspar	
J50	2059	FI-WB-03	Fine grained brown stained quartz, larger grains are transparent	noises
J57	2060A	FI-WB-05	Banded fine grained light brown qtz and med grained white felspar, 80% qtz, no mafic	
J58	2060B	FI-WB-05	80% fine grained qtz, 10% white felspar, 10% mafics	
J59	2050	FI-OK-09	Fine grained speckled pale grey granodiorite, 10% mafic	repeat
J60	2053	FI-OK-12	Semi translucent white qtz, yellowish, medium grainsize	
J61	2059	FI-WB-03	Fine grained brown stained qtz. Larger grains are transparent	storm noises
J63	2059	FI-WB-03	Fine grain brown stained qtz. Larger grains are transparent	Repeated J61

Field sample numbers are noted on each result and also cross referenced in the data table (Table6.3).Sample 2060 (WB-05) had two distinct zones, so I separated these as two subsamples, with suffix A and B and analyzed these separately. There was essentially no difference

between the two subsamples. Note that some samples had some outside interference and were re-analyzed (2050, 2059).

Table6.4.Decrepitation counts of fluid inclusion by baro-acoustic analytical method

TEMP	FI-OK-01 (2046)	FI-OK-02 (2047)	FI-WB-03 (2059,N)	FI-WB-03 (2059)	FI-WB-03 (2059,R)	FI-HO-04 (2057)	FI-WB-05 (2060A)	FI-WB-05 (2060B)	FI-HO-06 (2058)	FI-OK-07 (2048)	FI-OK-08 (2049)	FI-OK-09 (2050)	FI-OK-09 (2050,R)	FI-OK-10 (2051)	FI-OK-11 (2052)	FI-OK-12 (2053)	FI-OK-13 (2054)	FI-OK-14 (2055)	FI-OK-15 (2056)
110	3	10	1	12	3	1	4	2	1	12	6	22	24	7	10	9	19	40	5
120	2	3	3	31	3	1	10	13	18	7	11	2	22	4	7	11	74	37	25
130	3	14	23	21	9	2	12	7	5	16	22	36	22	0	7	13	75	69	10
140	6	10	4	9	16	1	7	28	20	21	29	26	12	1	12	9	125	78	20
150	10	43	17	11	3	16	16	0	18	7	67	27	4	2	34	12	215	123	34
160	15	103	11	11	6	14	17	8	9	26	102	19	4	9	36	64	275	102	60
170	3	127	24	4	6	13	7	14	28	24	118	31	11	1	23	17	377	96	38
180	2	251	1	10	1	5	6	5	6	32	210	12	2	49	51	21	474	154	45
190	6	341	1	14	5	17	12	25	34	29	354	69	3	10	54	16	484	236	66
200	9	419	4	1	2	13	17	31	38	40	446	16	2	3	92	28	429	218	84
210	12	626	9	36	1	14	7	33	40	21	500	44	0	59	134	44	503	308	80
220	5	802	6	58	3	27	14	44	118	39	591	39	1	1	200	83	472	460	144
230	10	1004	8	49	2	18	24	9	131	33	856	53	10	13	250	134	644	483	187
240	6	1089	5	41	19	29	36	32	164	23	936	64	4	6	331	188	657	528	234
250	12	1178	11	48	24	38	46	42	171	34	1103	50	19	6	410	206	763	533	357
260	20	1330	33	24	19	77	49	53	206	33	1178	37	5	9	506	292	884	540	482
270	23	1177	19	38	20	92	53	81	246	42	1336	49	12	8	555	367	1143	688	568
280	14	1159	26	25	26	62	59	84	263	53	1311	49	1	18	624	425	1050	659	637
290	30	1192	24	37	30	99	70	124	343	47	1368	89	3	12	620	464	1155	707	571
300	53	1034	33	38	31	107	85	118	314	50	1468	18	5	8	663	497	1272	829	608
310	76	970	34	22	24	84	91	145	290	61	1265	37	7	21	611	481	1575	819	558
320	74	847	89	36	33	92	118	182	376	72	1214	59	26	31	642	557	1659	829	538
330	71	766	241	49	43	84	143	248	359	76	1118	63	20	22	619	530	1782	820	596
340	71	862	270	57	102	92	172	312	384	110	1124	66	20	21	651	544	1854	867	709
350	74	870	182	64	70	87	220	440	426	107	1150	60	27	31	655	597	2145	1077	754
360	97	924	554	83	80	134	475	691	452	132	1033	82	43	25	704	583	2238	1071	838

370	112	897	728	115	73	145	634	871	490	184	1003	64	44	44	637	660	2251	1404	1103
380	155	1053	4496	91	107	171	843	1263	504	215	1092	143	54	91	790	721	2359	1502	1373
390	161	1243	1724	83	113	158	1332	1595	531	217	1150	182	107	120	876	729	2824	2181	1849
400	209	1295	138	154	146	168	1551	2078	601	319	1276	196	141	160	1006	773	2855	2722	2537
410	241	1559	243	198	198	242	1803	2639	734	317	1357	264	223	224	1142	840	2839	3353	2970
420	298	1902	354	201	293	284	2037	2817	777	372	1650	475	237	355	1148	895	3247	3750	3556
430	303	1847	388	285	291	341	2515	3004	818	473	1814	459	307	429	1248	839	3400	3994	3726
440	422	2085	402	330	354	469	2767	3469	1022	428	2018	603	380	455	1437	973	3577	3996	4393
450	449	1996	394	299	377	616	2882	3312	1171	687	2250	806	350	494	1505	992	3173	4029	4092
460	520	1966	397	371	314	713	2811	3396	1329	673	2310	861	281	382	1833	1111	3386	4059	4005
470	429	1961	328	517	341	720	2538	3110	1166	698	2425	905	260	361	1643	972	3238	3603	3825
480	435	1903	289	501	342	822	2161	2846	1235	695	2317	967	209	287	1560	958	3019	3083	3413
490	371	1854	261	298	306	892	1974	2589	1219	646	2187	957	183	213	1601	999	3101	2936	2948
500	387	1878	222	228	285	744	1698	2487	1108	599	2058	996	143	196	1405	901	2963	2561	2611
510	363	2119	240	256	232	601	1504	2120	931	553	2258	955	145	193	1285	860	3125	2200	2321
520	340	1976	194	236	222	561	1267	2160	869	720	2046	782	133	126	1217	825	2858	1795	1970
530	327	2094	183	186	207	456	1222	1899	728	744	2159	802	108	133	1063	760	2807	1537	1652
540	270	1999	200	193	232	486	1011	1758	670	971	1983	885	95	153	1119	800	2512	1329	1425
550	280	2390	187	228	202	395	809	1551	689	876	1948	1037	101	142	1043	820	2573	1262	1248
560	341	2599	185	209	253	322	792	1444	683	956	2277	765	134	172	1016	1055	2872	1253	1307
570	321	3186	259	279	274	332	666	1208	675	954	2457	621	132	183	1144	1138	2870	1284	1261
580	459	8411	1367	886	1023	756	879	1360	2101	1627	5477	1168	402	411	2346	2840	3575	2711	2307
590	688	10952	1735	1954	1434	1033	1451	1366	2915	1893	9261	1390	571	801	3767	5254	3942	5055	4378
600	479	7493	97	1156	704	394	732	883	1080	1335	7719	923	282	410	3637	2682	2643	3364	3081
610	275	672	11	1110	107	166	271	627	214	1014	3126	631	120	78	2158	548	1846	467	1311
620	254	130	28	931	133	132	182	547	206	789	267	534	43	97	857	259	1812	120	309

The peak at 590 C is due to the alpha-beta transition of quartz and has no meaning in understanding the hydrothermal fluid system. Only the lower temperature peaks are relevant in understanding the gas content and temperature of the fluid system.

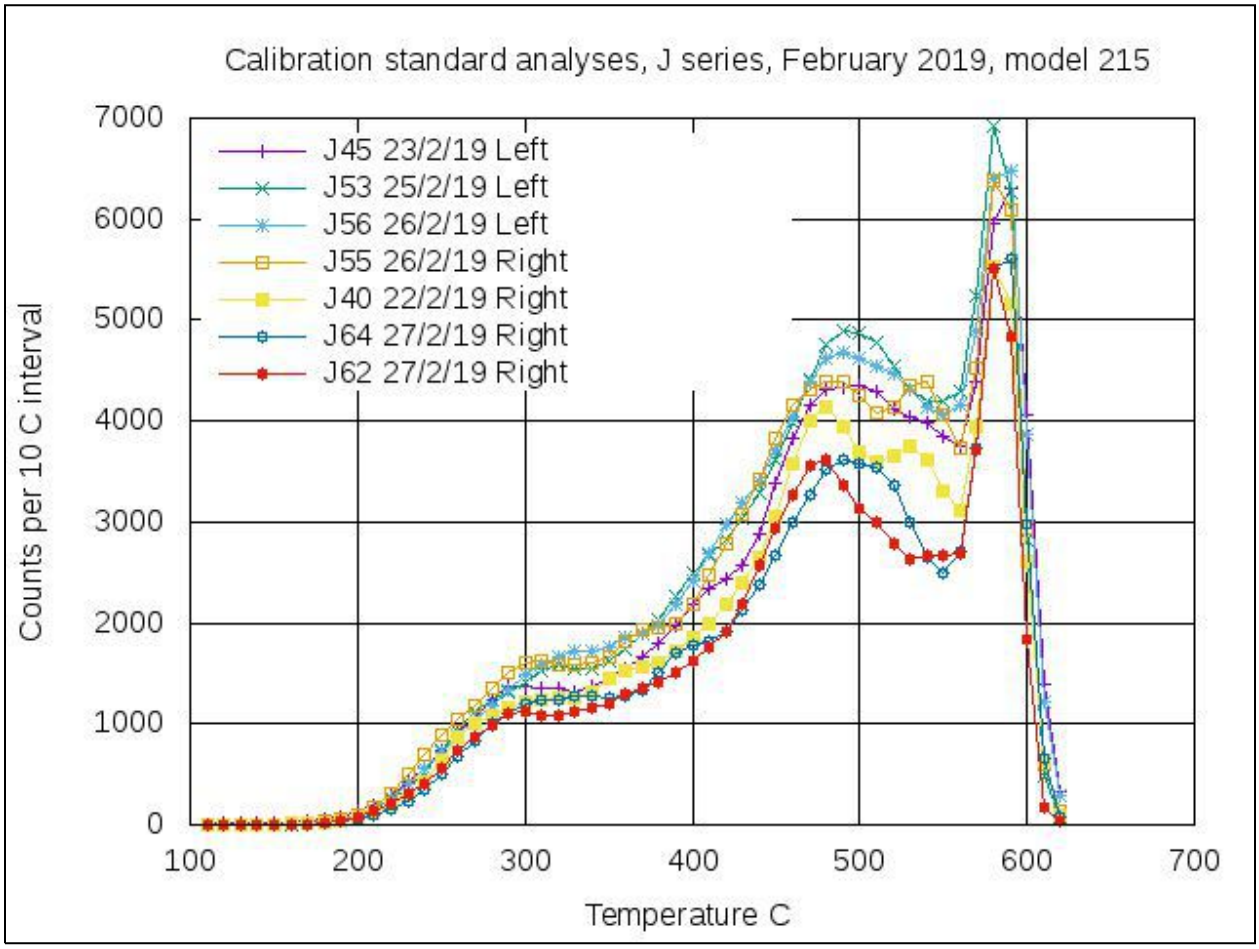

Figure6.1. Calibration standard analyses of Burlinson laboratory, model 215

Graph of Burlinson laboratory are used for calibration to understand the reproducibility of the data (Figure 6.1).

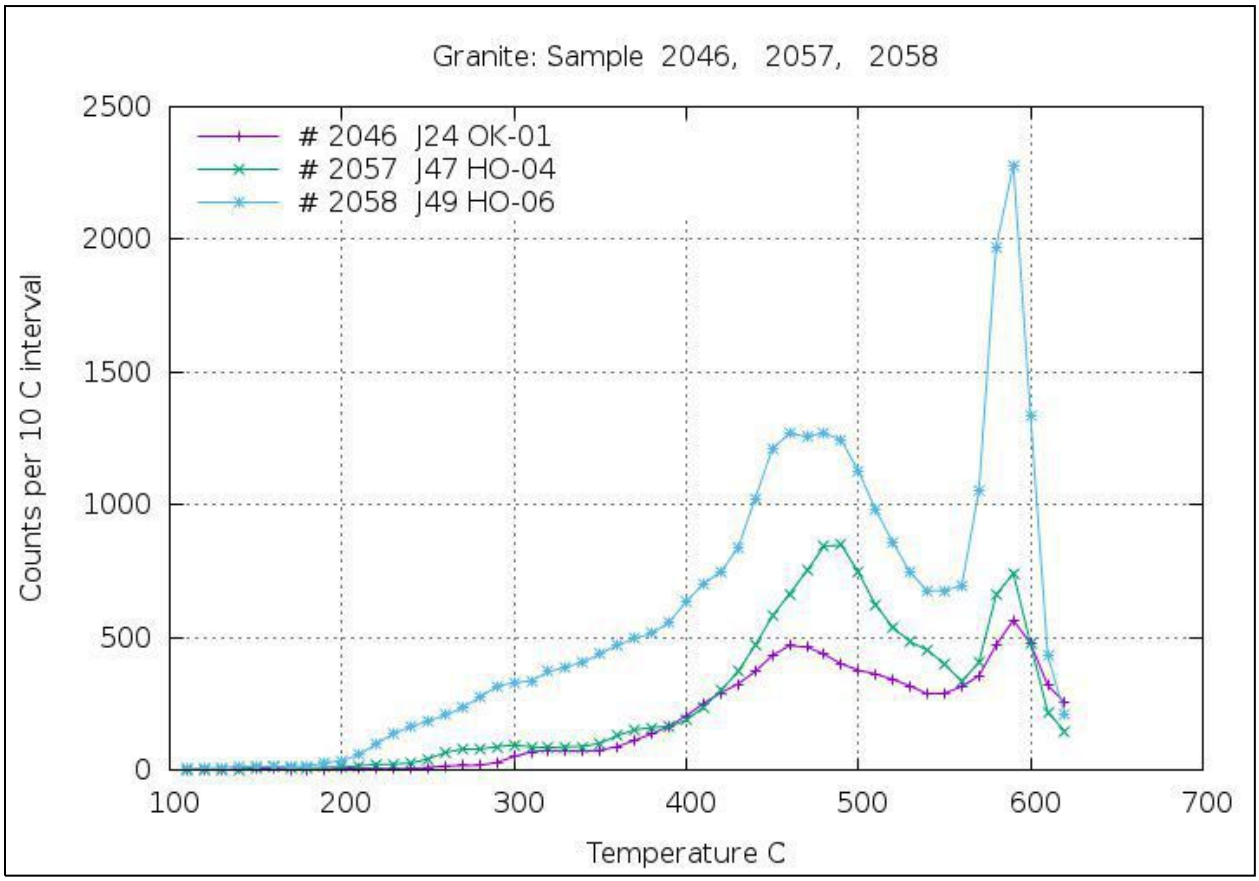

Figure6.2.Granite samples verification for FI decrepitation values

Granitic samples from Horoto and Wayu Boda prospect areas lack low temperature decrepitation, indicating the absence of CO_2 rich fluids, by suggesting the occurrence of magmatic hydrothermal fluids.

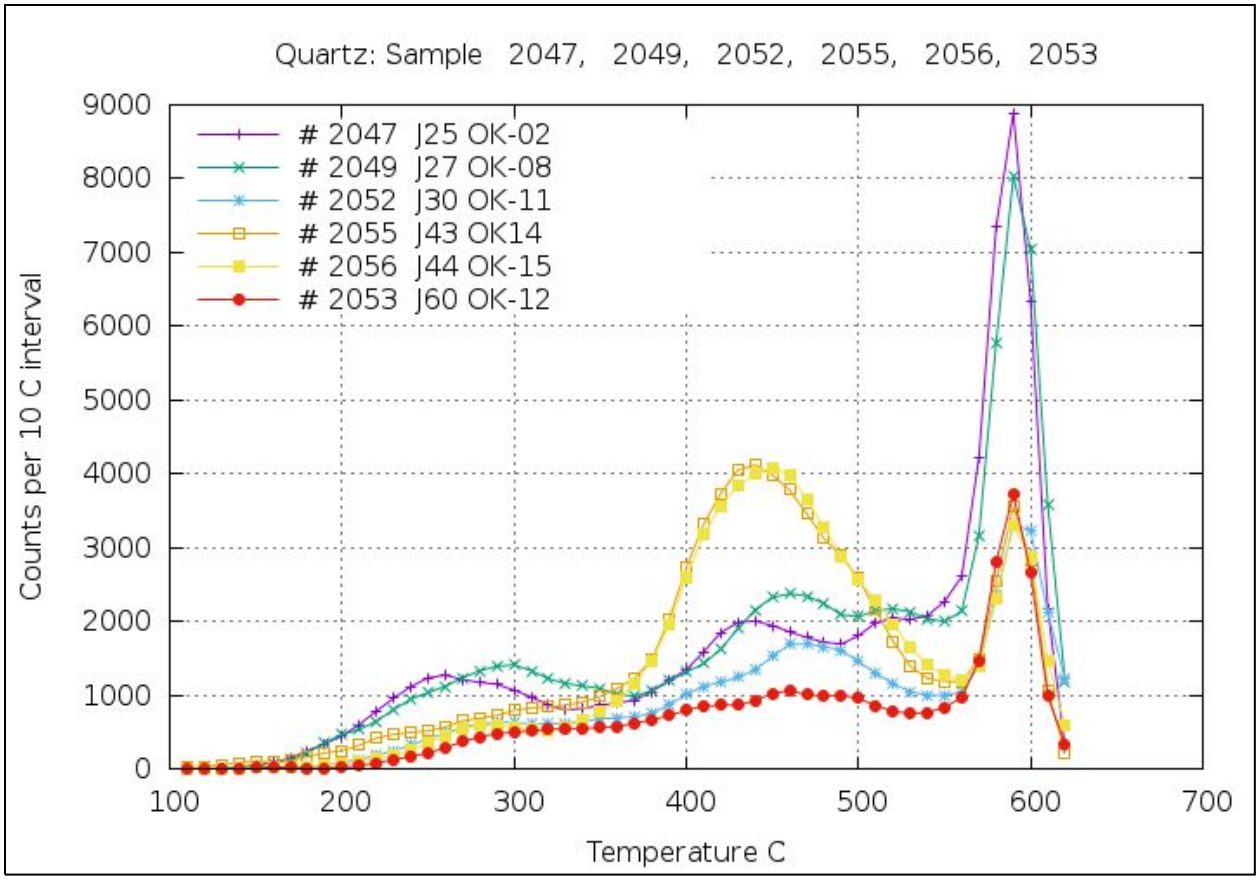

Figure6.3.Quartz samples verification for FI decrepitation values

The quartz vein samples plotted above (Figure6.3) contain trace amounts of CO_2 rich fluids, explaining minor influence of metamorphic hydrothermal fluid. This is a justification for the coexistence of intrusive related and shear controlled mineralization of gold and base metal in the same granodioritic host rock. The host rock exhibit disseminated hypothermal whereas the quartz veins are structurally controlled mesothermal mineralization.

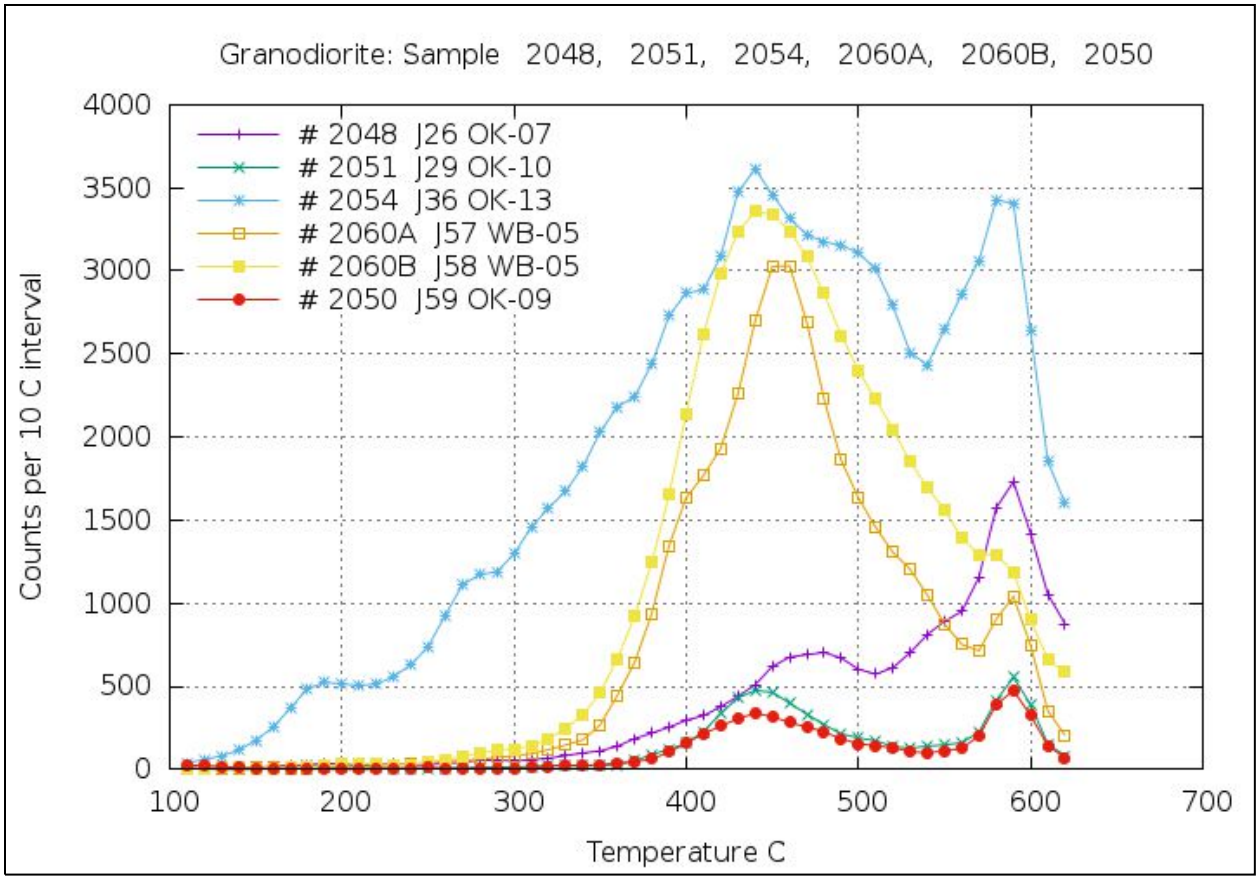

Figure6.4.Granodiorite samples verification for FI decrepitation values

Five granodiorite samples from Okote and Wayu boda prospect areas lack low temperature decrepitation and CO_2 rich fluid inclusions, explaining the dominance of magmatic hydrothermal fluid. There are some interesting variations with dual decrepitation peaks at about 440^0 C, suggesting multiple quartz formation events and hence polyphase mineralization.

CHAPTER SEVEN

7. DISCUSSION AND CONCLUSION

7.1. Discussion

Intrusive related gold (Lang & Baker, 2001) is generally hosted in granites, porphyry or rarely dikes. Intrusive related gold usually also contains copper, and is often associated with tin and tungsten, and rarely molybdenum, antimony and uranium. Intrusive-related gold deposits rely on gold existing in the fluids associated with the magma (White, 2001), and the inevitable discharge of these hydrothermal fluids into the wall-rocks (Lowenstern, 2001).

Source of fluid and gold: The generation of oxidized I-type granite magmas is associated with melting processes adjacent to subducted oceanic crust. Porphyry type deposits can be explained in terms of a body of magma with a relatively low initial H_2O content (inherited from the fluid absent melting of an amphibolitic protolith) rising to high levels in the crust before significant crystallization takes place. The hot and saline aggressive juvenile hydrothermal fluid leaches and concentrates the metals (Au and Cu in this case) along the way to a near surface depositional chamber.

Transport and Deposition site of Gold: It is considered likely that some melt fractions from high level magma chamber will be tapped off and extrude on the surface. These fractions will crystallize to form volcanic and subvolcanic (porphyry) suites of rocks whose compositions will not be highly differentiated (i.e. granodioritic or rhyodacitic) because of the low degree of fractionation that has taken place prior to extrusion. Because the magma is emplaced at low load pressures the saturation water content will be relatively low and probably not significantly different from the initial water content. Vapor-saturation will, therefore, occur early in the crystallization sequence, essentially due to “first boiling.” Even though the metals are compatible elements in a crystallizing granitic melt (sequestration of the metal into accessory sulfide phases and biotite result in Dmetals crystal/melt > 1), the lack of crystallization means that very little of the metal will have been removed from the melt by the time water-saturation occurs. The vapor phase, by contrast, is characterized by high Cl^- concentrations and it will, therefore, efficiently scavenge the metals from the silicate melt (Laurence Robb, 2005). In this setting, therefore, a high level granodioritic I-type magma will exsolve an aqueous fluid phase that is highly enriched

in metals, and form a typical porphyry deposit which is in good agreement with the granodiorite gold mineralization of the study area.

Precipitation Mechanism: Fluid mixing and dilution is an important precipitation mechanism in volcanic deposits like porphyry (Au & Cu) and epithermal (Au & Ag). This is especially important when hot, metal laden ore fluid mingles with cooler and more dilute solution. This leads to cooling of the hotter and destabilization of the existing complex. In porphyry type deposit mixing of juvenile and meteoric fluids resulted destabilization of chloride complex by precipitating gold and formation of concentric potassic and pyllic alteration zoning (Solomon, 2015). Hence mixing of hotter magmatic and cooler meteoric fluids with distinct T, P, PH and reduction oxidation characteristics is the precipitation mechanism of granodiorite hosted Au & Cu deposit of the study area.

7.2. Conclusion

Rock petrography explained the coexistence of secondary copper minerals (Malchite and Azurite) and gold in granite-granodiorite intrusive which is a typical characteristic of porphyry deposits. The granitoids exhibit disseminated mineralization throughout the lithology without showing any structural control. The ore minerals are undefromed and massive pyrite, pyrothite, chalcopyrite, malachite and azurite.

Combined geochemistry data revealed the mineralized host rock is granodiorite originated from primary melt by direct melting of hydrous oceanic crust and the mantle wedge overlying the conveyor belt. The hydration of oceanic crust is due to the introduction of water at the conveyor belt that initiated the melting of basaltic rocks and generation of andesitic, latter contaminated by mantle wedge during its ascent at subduction zone.

Sample for petrographic study clearly outlined that the fluid inclusion is Type-I which is characterized by moderately saline inclusion containing two phases, which suggests magmatic hydrothermal fluid which is evidenced by 10-15% vapor constitute and lack of CO_2 segregation.

Granitic samples from Horoto and Wayu Boda prospect areas lack low temperature decrepitation, indicating the absence of CO_2 rich fluids, by suggesting the occurrence of juvenile hypothermal fluids. Okote quartz samples contain trace amounts of CO_2 rich fluids, explaining minor influence of metamorphic hydrothermal fluid. There are some interesting variations with dual decrepitation peaks at about 440^0 C suggesting multiple quartz formation events and hence polyphase mineralization.

REFERENCES

Abdelselam and Stern (1997). Sutures and shear zones in Arabian-Nubian Shield. Journal of African Earth Sciences, Vol. 23, pp 289-310.

Abdelselam,Lulu, Tadesse and Bedru (2008). Terrane rotation during the East African Orogeny, Evidence from BulbulShear Zone, South Ethiopia.Gondwana Research 14(2008),497-508.

Abu Wube (2005). Mineralization and associated structures of Okote prospect, Southern Ethiopia. Msc. Thesis, Addis Ababa University ,pp iii.

Alecto Minerals plc (2013). Positive Exploration update, Wayu Boda Gold project, Ethiopia: www.alectominerals.com

Amenti (1996). The Precambrian of Southern Ethiopia, Addis Ababa, Ethiopia. Ethiopian Institute of Geological Surveys, Addis Ababa, Ethiopia.

A.N. Clay (2012). A Scoping Study on the Okote Gold Project by Venmyn Independent Projects (PTY) Limited,unpublished technical report. National Mining Corporation, Addis Ababa, Ethiopia, pp xiii of executive summary and pp 49.

A.Asrat (2001). The Precambrian Geology of Ethiopia, Africa Geoscience Review, Vol 8,No. 3,pp.271-288.

Begashaw, Zemen, Zerihun and Julio (1996). Neoproterozoic zirconium-depleted boninite and tholeiitic series rocks from Adola, southern Ethiopia. Precambrian research 80 (1996)261-279.

Bodnar (2003). Fluid Inclusions Analysis and Interpretation. Mineralogical Association of Canada.

Bruce W. Chappell, Colleen J.Bryant and Doone Wyborn (2012). Peraluminous I type granites of Lachlan Fold Belt. ScienceDirect, Lithos. Volume 153 15 November 2012, Pages 142 153.

Burlinson K. (2012). An Overview of information and results on using fluid inclusion information in mineral exploration. Burlinson Geochemical Services Pty. Ltd. Winnellie, NT, Australia http:\\appliedminex.com

Chappell & White (1974); Australian Journal of Earth Sciences (2001) **48**, 489 499.

Chris Peg (2002). Evaluation of gold exploration results of Okote project, unpublished technical report (NMiC), Addis Ababa, Ethiopia,pp1-4.

Cox K.G., Bell J.D. and Pankhurst R.J. (1979). The interpretation of igneous rocks. George, Allen and unwin, London.

Dandena & Walter (1999). Constraints on interpretation of geochemical data for gold exploration in multiply deformed andmetamorphosed areas: an example from Legadembi gold Deposit, Southern Ethiopia.Journal of Africa Earth Sciences, Vol.29, No.2, pp367-380.

Danilo Jelenc (1959). Adola Gold Placers and Nickel-Chromium Ore Deposits, Southern Ethiopia.

Debele, D. and Koerbel, C. (2004). Geochemistry, alteration and genesis of gold mineralization in Okote area, Southern Ethiopia.Geochemical Journal. 38: 307-331pp.

Ethiopian Institute of Geological Surveys DawaDigati primary gold exploration and development project (1995). Report on mineral exploration in DawaDigati area, Adola Ore district, southern Ethiopia, EIGS, Addis Ababa, Ethiopia.

Ethiopian Institute of Geological Surveys/UNDP Project (1993). Final report on mineral exploration in Adola area, Sidamo, EIGS, Addis Ababa, Ethiopia.

Fritz and Abdelselam (2013). Orogen styles in the East African Orogen: A Review of Neoproterozoic to Cambrian tectonic evolution. Journal of African Sciences 86(2003) 65-106.

Gass (1982). The late Proterozoic rocks of NE Africa ,NE-Africa & Ethiopia.

Ghebreab (1992). The geological evolution of the Adola Precambrian greenstone belt,Southern Ethiopia. *Journal of African Earth Sciences,* Vol. 14, No. 4, pp. 457-469.

Gilboy (1970). The Geology of Gariboro Region of Southern Ethiopia, Research Institute of African Geology, Department of Earth Sciences, The University of Leeds.

Ginchile (1991). Structure, Metamorphism and Tectonic setting of a gneissic terrain, The Sagan Aflata area.Ottawa-Carleton Geoscience center and the University of Ottowa.

Ginchile and Fyson (1993). An inference of the tectonic setting of the Adola Belt ofSouthern Ethiopia from the geochemistry of magmatic rocks *Journal of African Earth Sciences,* Vol. 16, No. 3, pp. 235-246.

Hamrla (1977). The Adola Gold Field, Geology and Genetic Hypothesis, Ethiopia.Geologija 20,pp 247-282.

Harker A. (1909). The natural history of igneous rocks, Methuen, London.

Haskin M.A. and Frey F.A. (1966). Dispersed and not-so-rare earths. Science, 152, 299-314.

Hugh. R. Rollinson (1993). Using Geochemical Data. Evaluation, Presentation, Interpretation; Pearce Educational Limited, Longman Group UK Limited, England. *PP145-149*.

Kazmin,V. (1972). Geology of Ethiopia; explanatory note to the geological map of Ethiopia, (1:2,000,000). Ministry of Mines, Addis Ababa, Ethiopia, 14 pp.

Kazmin V. (1975b). The Precambrian of Ethiopia and some aspects of the Geology of Mozambique Belt, Ethiopia.

Kazmin V. (1978). The Ethiopian Basement: Stratigraphy and possible manner of evolution, Ethiopia.

Kenea, Admassie, Tsegaye & Tadesse (2003). Report on the result of copper prospecting work at Gewale, Horoto and Wachile areas (in Southern Oromia regional state). **EMRDC,** Mineral Exploration and Evaluation Department.

Kozyrev (1985). Regional Geological and Exploration Work for Gold and other minerals in the AdolaGoldfields, Volume II. Regional Geological Mapping and prospecting Ethiopia, Ministry of Resources Development Corporation, Addis Ababa.

Kuno H. (1968). Differentiation of basalt magmas. In: Hess H.H. and Poldervaart A.(eds.), *Basalts: The Polderlvaart treatise on rocks of basaltic composition*, Vol.2, Interscience, New York, pp.623-688.

Lang & Baker (2001); as cited D.I.Groves etal.,Mineral deposits and earth evolution; pp80.

Laurence Robb (2005), Introduction to Ore Forming Process, pp101-103.

Lulu T. (2006). Metamorphism and gold mineralization, Kenticha–Katawicha area, Adola Belt, Southern Ethiopia. Journal of Africa Earth Sciences 45(2006) 16-32.

Mulugeta A. & Andrew (1997). Geochemistry of meta-igneous rocks from Southern Ethiopia: a new insight into Neoprotozoic tectonics of northeast Africa. Journal of Africa Earth Sciences, Vol.24, No.3, pp351-370.

National Mining Corporation (1997). Final Report for the first year of the initial Gold exploration period, unpublished technical report. National Mining Corporation, Gold Project, Addis Ababa.

National Mining Corporation (2004). Summary of Exploration work on DawaDigati gold exploration project, southern Ethiopia, unpublished technical report. National Mining Corporation, Addis Ababa, Ethiopia.

Pearce,J.A. and Cann, M.J. (1973); Tectonic setting of basic volcanic rocks determined using trace elements analysis. Earth Planet. Sci. Lett.19,290-300.

Pearce, J.A. and Parkinson, I.J., 1993, Trace element models for mantle melting: application to volcanic arc petrogenesis; in Prichard, H.M., Alabaster, T., Harris, N.B.W., and Neary, C.R., eds., Magmatic Processes and Plate Tectonics, Geological Society Special Publications, no. 76, p. 373-403.

Pr. I.J. Basson (2006). MGSSA, MSEG Tect Geological Consulting ,Structural analysis of selected areas in the DawaDigati prospect area, Adola gold belt, Ethiopia and recommendations on data formats for their evaluation, unpublished technical report. National Mining Corporation, Addis Ababa, Ethiopia.

R.J. Stern, Kamal A. Ali, Mohamed G. Abdelsalam, Simon A. Wilde, Qin Zhou (2012).U–Pb zircon geochronology of the eastern part of the Southern Ethiopian Shield. Precambrian Research 206– 207 (2012) 159– 167.

Roedder and Budnar (1997). Fluid Inclusion Studies of Hydrothermal ore Deposits. Harvard University and Virginia Polytechnic Institute and State University. Chapter 13.

Saunders A.D. and Tarney J. (1984). Geochemical characteristics of basaltic volcanism within back-arc basin. In: Kokelaar B.P. and Howells M.F. (eds.) *Marginal basin geology*, Spec. Pub. Geol. Soc. London 16, pp.59-76.

Sha L.K. and Chappel B.W. (1999). Apatite chemical composition, determined by electron microprobe and laser-ablation inductively coupled plasma mass spectrometery, as a probe into granite petrogenesis. *Geochemica et Cosmochemica Acta* 63, 3861-3881.

Shand S.J. (1943). The eruptive rocks: 2nd edition , John Wiley, New York, pp444.

Shiferaw D., Marchuk, Y. and Evdokimove, V., (1987). Summary of Geology and Mineral Potential of the Adola Area. EMRDC, Addis Ababa.

Schmerold, R.M., (1988). Report on field trip to Adola Gold Field. Training for mineral exploration project, Ethiopia Institute of Geological Surveys, unpublished technical report.

Seife M. Berhe (1990). Ophiolites in Northeast and East Africa: implications for Proterozoic crustal growth. *Journal of the Geological Society, London,* Vol. 147, 1990, pp. 41-57.

Solomon G. (2015). Geochemistry, Alteration and Genesis of Granodiorite hosted Gold Mineralization, Okote, Southern Ethiopia.

Solomon T. (1999). Geology and Gold Mineralization in the Pan-African Rocks of the Adola area, SouthernEthiopia.Gondwana Research, Vol.2, No.3, pp 439-447.

Solomon T. (2004). Genesis of the Shear Zone-related Gold Vein Mineralization, LegaDembi

Gold Deposit, Adola Gold Field, Southern Ethiopia.Gondwana Research, Vol.7, No.2, pp 481-488.

Sun S.S. (1980). Lead isotopic study of young volcanic rocks for mid-ocean ridges, ocean islands and island arcs , ***Phil. Trans. R. Soc., A297, 409-445***.

Sun and MacDonough (1989). In A. D. Saunders and M. J. Norry (eds.), Magmatism in the Ocean Basins. Geol. Soc. London Spec. Publ., **42**. pp. 313-345.

Tadesse & Melaku (2002). Structural evidence for the allochthonous nature of the Bulbul terrane in Southern Ethiopia: A west verging thrust nappe. Journal of African Earth Sciences 34 (2002) 85-93.

Tadesse Y. (2003). Chemical U-Th-total Pbisochron ages of zircon and monazitefrom granitic rocks of the Negelearea.J earth Planet. Sci. Nagoya Univ., Vol.50.,1-12.

TadesseY., Mamoru A. and Mokoto T., (2004). P-T Conditions of Metamorphism in the Neoproterozoic Rocks of the Negele Area, Southern Ethiopia.*Gondwana Research,* **I?***7, No. 2, pp. 489-500.*

Wilkinson (2002). Fluid Inclusions in hydrothermal ore deposits.Lithos 55(2001) 229-272.

Wilson (1989). The chemical classification and nomenclature of plutonic rocks using total alkali versus silica; after Cox-Bell-Pank (1979)

Winter (2001) An Introduction to Igneous and Metamorphic Petrology. Prentice Hall.

Woldehaimanot and Behrmann(1995). A study of metabasite and metagranite chemistry in Adola Region, southern Ethiopia.Journal of African Earth Sciences, Vol 21, No. 3, pp.459-476.

Wood D.A. (1980). The application of a Th-Hf-Ta diagram to problems of tectonomagmatic classification and to establishing the nature of crustal contamination of basaltic lavas of the British Tertiary volcanic province. *Earth planet, Sci,Lett*.,50, 11-30.

Worku, H. (1996). Structural control and metamorphic setting of the shear zone-related Au vein mineralization of the Adola Belt (southern Ethiopia) and its tectono-genetic development.Journal of African Earth Sciences, Vol 23, No. 3, pp.383-409.

Worku, H and Schandelmier, H. (1996). Tectonic evolution of the NeoproterozoicAdola belt of Southern Ethiopia: evidence for a Wilson cycle process and implication for oblique plate collision. Precambrian Research. 77:179-210pp.

Yibas, B., Reimold, W. U., Armstrong, R., Koeberl, C., Anhaeusser, C. R. and Phillips D. (2002). Tectonostratigraphy, granitoid geochronology and geological evolution of the Precambrian rocks of Southern Ethiopia.Journal of African Earth Sciences.34:57-84

Yibas, Reimold, W. U., Armstrong, R., Koeberl, C. (2003). Geochemistry of the mafic rocks of the ophiolitic fold and thrust belts of Southern Ethiopia: constraints on the tectonic regime during the neoproterozoic (900-700 Ma). Precambrian Research 121 (2003),157-183.